

ผลของไตรเอทานอลามีนในสารหล่อลื่นสำหรับกระบวนการขัดหัวอ่าน-เขียนฮาร์ดดิสก์ไดรฟ์

Studying effect of triethanolamine in lubricant for using in lapping slider head process



โดย  
นาย ปิยนันท์ แดงเนียม

ภาควิชาเคมี  
คณะวิทยาศาสตร์  
จุฬาลงกรณ์มหาวิทยาลัย

ปริญญาวิทยาศาสตรบัณฑิต  
ภาควิชาเคมีคณะวิทยาศาสตร์

จุฬาลงกรณ์มหาวิทยาลัย

ปีการศึกษา 2557

เรื่อง ผลของไตรเอทานอลามีนในสารหล่อลื่นสำหรับกระบวนการขัดหัวอ่าน-เขียนฮาร์ดดิสก์ไดรฟ์  
โดย นาย ปิยนันท์ แดงเนียม  
ได้รับอนุมัติให้เป็นส่วนหนึ่งของการศึกษา  
ตามหลักสูตรปริญญาวิทยาศาสตรบัณฑิต ภาควิชาเคมี  
คณะวิทยาศาสตร์ จุฬาลงกรณ์มหาวิทยาลัย

คณะกรรมการสอบโครงการ

.....ประธานกรรมการ  
(ผู้ช่วยศาสตราจารย์ ดร. ปกรณ์ วรรณสุภากุล)  
.....รองประธานกรรมการ  
(อาจารย์ ดร. ดวงกมล ตุงคะสมิต)  
.....กรรมการ  
(อาจารย์ ดร. สกฤษ สุข อุ่นอรุณทัย)

รายงานฉบับนี้ได้รับความเห็นชอบและอนุมัติโดยหัวหน้าภาควิชาเคมี

.....  
(รองศาสตราจารย์ ดร. วุฒิชัย พาราสุข)  
หัวหน้าภาควิชาเคมี  
วันที่ 21 เดือน ๗.ค. พ.ศ. 2558

คุณภาพของการเขียนรายงานเล่มนี้อยู่ในระดับ



ดีมาก



ดี



พอใช้

ชื่อโครงการ ผลของไตรเอทานอลามีนในสารหล่อลื่นสำหรับกระบวนการขัดหัวอ่าน-เขียนฮาร์ดดิสก์ไดรฟ์  
ชื่อนิติโครงการ นาย ปิยนันท์ แดงเนียม เลขประจำตัว 5433113523  
อาจารย์ที่ปรึกษา อาจารย์ ดร. ดวงกมล ตุงคะสมิต  
ภาควิชาเคมี คณะวิทยาศาสตร์ จุฬาลงกรณ์มหาวิทยาลัย ปี 2557

### บทคัดย่อ

ปัญหาที่พบในกระบวนการขัดหัวอ่าน-เขียนในอุตสาหกรรมฮาร์ดดิสก์ไดรฟ์คือการใช้เวลาในการขัดชิ้นงานที่นานเกินไปส่งผลให้การผลิตงานล่าช้า ดังนั้นแผนกพัฒนาคุณภาพหัวอ่าน-เขียนของบริษัทเวสเทิร์นดิจิตอลมีความสนใจที่จะศึกษาสารเติมแต่งในสารหล่อลื่นที่ใช้ในกระบวนการขัดเพื่อที่จะลดเวลาในการขัดชิ้นงาน จากผลงานวิจัยพบว่าไตรเอทานอลามีนที่เป็นสารเติมแต่งในเอทิลีนไกลคอลซึ่งใช้เป็นน้ำมันหล่อลื่นพื้นฐานนั้นช่วยลดเวลาในการขัดชิ้นงานดังที่งานวิจัยนี้จะศึกษาเกี่ยวกับผลกระทบของไตรเอทานอลามีนต่อกระบวนการขัดการทดลองนี้แบ่งออกเป็น 4 ส่วนโดยที่ ส่วนที่ 1 คือการตรวจสอบสมบัติทางกายภาพและเคมีของน้ำมันหล่อลื่น ในส่วนที่ 2 ทำการทดลองโดยใช้สไลด์คอร์บาร์นำไปผ่านกระบวนการขัดและทดลองโดยการจุ่มในสารหล่อลื่นโดยใช้สารหล่อลื่นที่มีปริมาณของไตรเอทานอลามีนต่างกันที่ 0%, 3%, 6% และ 10%wt. ในเอทิลีนไกลคอลในส่วนที่ 3 ทำการทดลองโดยใช้แผ่นอะลูมินาไทเทเนียมคาร์ไบด์เคลือบด้วยอะลูมินาออสซิลฐานซึ่งใช้เป็นตัวแทนองค์ประกอบหลักของสไลด์คอร์บาร์ โดยทำการจุ่มในสารหล่อลื่นที่มีประกอบด้วย 6%ไตรเอทานอลามีน ตรวจสอบพื้นผิวโดยกล้องจุลทรรศน์ กล้องจุลทรรศน์แรงอะตอมและตรวจสอบความเรียบของพื้นผิว ในส่วนที่ 4 นั้นศึกษาปฏิกิริยาเคมีระหว่างของแข็งอะลูมินาซึ่งใช้เป็นตัวแทนของสไลด์คอร์บาร์และไตรเอทานอลามีนในเอทิลีนไกลคอลโดยตรวจสอบเอกลักษณ์ของสารที่ได้หลังทำปฏิกิริยาด้วยเทคนิครามาน สเปกโทรสโกปีและ  $^1\text{H}$  NMR สเปกโทรสโกปี นอกจากนี้ยังมีการศึกษาผลของไตรเอทานอลามีนต่อโลหะผสมโคบอลต์ซึ่งเป็นองค์ประกอบย่อยของสไลด์คอร์บาร์โดยวิธีโพเทนทิโอสแตติกสโพลาริเซชันจากผลการทดลองสรุปได้ว่าไตรเอทานอลามีนช่วยลดเวลาในการขัดงานโดยกำจัดอะลูมินาจากพื้นผิวผ่านการเกิดสารเชิงซ้อน

คำสำคัญ : กระบวนการขัด, ไตรเอทานอลามีน, สไลด์คอร์บาร์, อะลูมินา

Title: Studying effect of triethanolamine in lubricant for using in lapping slider head process

Student name: Mr. Piyanan Dangnearm ID: 5433113523

Advisor: Dr. Duangamol Tungasmita

Department of Chemistry, Faculty of Science,  
Chulalongkorn University, Academic Year 2014

### Abstract

A problem in lapping slider head process in hard disk drive industry is spending a long lapping time leading to slow production. Therefore, slider fabrication development group of Western digital Co, Ltd has been interested in studying on some additives in lubricant using in lapping process to decrease lapping time. The research found that triethanolamine (TEA), one of the additives in ethylene glycol (EG) base stock helps reduce lapping time. Hence, this project studied on an effect of TEA in lapping process. The experiments were divided into 4 parts. The first part of experiment was testing physical properties of lubricants. The second part, experiments were done by using stripe slider bars in lapping and dipping with lubricants containing 0%, 3%, 6% and 10%wt. of TEA in EG. The third part, alumina titanium carbide (AlTiC) coupon coated with amorphous alumina as representative of major component in slider bar were dipped in 6%wt. of TEA and then characterized by optical microscopy, atomic force microscopy (AFM) and roughness test. The fourth part was study on the chemical reaction of solid alumina and TEA and characterization with Raman and  $^1\text{H-NMR}$  spectroscopy. Furthermore, the study on effect of TEA on cobalt-iron alloy which is minor component of slider bar was done by using potentiodynamic polarization technique. The results showed that TEA can reduce lapping time by removing alumina part of slider bar by Al-TEA complex formation.



Keyword: Lapping process, Triethanolamine, Slider bar, Alumina

## ACKNOWLEDGEMENT

I wish to express my honest gratitude to my advisors: Dr. Duangamol Tungasmita, Dr. Laddawan Supadee, Assistant Professor Dr. Sukkaneste Tungasmita, Mr.Chakkrit Supavasuthi and Mr. Benjie Fernandez for their guidance, support and providing me an opportunity to do my internship and project at Western Digital Co. Ltd. This project would not be completed if I lacked of guidance and encouragement from them. Moreover, I would like to thank Assistant Professor Dr.Pakorn Varanusupakul and Dr. Sakulsuk Unarunotai for devoting time being my committees.

Furthermore, I also would like to acknowledge the co-operation of other staff member who gave a consult for me, study basic knowledge and train some instruments. They make me be a proficient. I got many experiences while doing the internship here. I also thank to zeolite research group for helping on many thing in this project.

In addition, I would like to gratefully and sincerely thank my friends for support and willingness to spend some times with me to give some advice. And that it's indispensable, that is, my parents to take care and foster me for all of my life. Finally, I would like to thank myself for paying attention and good learning as a result of accomplishing this project.



ภาควิชาเคมี  
คณะวิทยาศาสตร์  
จุฬาลงกรณ์มหาวิทยาลัย

## CONTENTS

	<b>Page</b>
Abstract (English)	C
Abstract (Thai)	D
Acknowledgement	E
Contents	F
Contents of figures	G
Contents of tables	H
Contents of appendix	I
Lists of abbreviation	J
<b>1. Introduction</b>	<b>1</b>
1.1 Background	1
1.2 Theory	2
1.3 Research limitation	16
1.4 Literature review	16
<b>2. Experimental</b>	<b>19</b>
2.1 Lapping experiments	22
2.2 Dipping test	22
2.3 Corrosion test of CoFe with TEA concentration effect	24
2.4 Physical and chemical properties measurement	25
2.5 Alumina powder and TEA reaction	27
2.6 Characterization	28
<b>3. Result and discussion</b>	<b>29</b>
3.1 Lapping experiments	29
3.2 Dipping test (Strip sample)	30
3.3 Corrosion test of CoFe with TEA concentration effect	32
3.4 Physical and chemical properties measurement	33
3.5 Characterization	35
<b>4. Conclusion</b>	<b>47</b>
Reference	48
Appendix	52
VITA	56

## Contents of figures

Figure		Page
<b>Figure 1</b>	Schematic views and real device of slider-disk interface	2
<b>Figure 2</b>	Thin film head process. (a) Wafer (b) Slider bars	3
<b>Figure 3</b>	Brief production of thin film head	4
<b>Figure 4</b>	Microstructure of TiC (gray) is dispersed in the Al <sub>2</sub> O <sub>3</sub> matrix (black)	5
<b>Figure 5</b>	Schematic structure of amorphous aluminum oxide (top) and crystalline $\alpha$ -Al <sub>2</sub> O <sub>3</sub> (bottom)	6
<b>Figure 6</b>	Schematics of lapping composition.	7
<b>Figure 7</b>	Lapping plates	8
<b>Figure 8</b>	Mechanisms of abrasive wear	9
<b>Figure 9</b>	(a) Abrasives and diamond slurry (b) Lubricants	10
<b>Figure 10</b>	Hydrodynamic lubrication diagram	11
<b>Figure 11</b>	Boundary lubrication diagram	11
<b>Figure 12</b>	Elasto-hydrodynamic diagram	12
<b>Figure 13</b>	Structure of ethylene glycol	15
<b>Figure 14</b>	Structure of triethanolamine	15
<b>Figure 15</b>	Sapphire removal rate and viscosity as a function of particle to dispersant ratio	17
<b>Figure 16</b>	Schematic of Slider head components	20
<b>Figure 17</b>	Lapping components (a) ASL 200 fine lap machine (b) diamond particle embedded on Sn-Bi plate (c) Lubricant	22
<b>Figure 18</b>	Slider bars were dipping in prepared solutions	23
<b>Figure 19</b>	Coupons were dipping in prepared solutions	23
<b>Figure 20</b>	Flatcell tool	24
<b>Figure 21</b>	Diagram of corrosion test tool	25
<b>Figure 22</b>	Eutech Instruments pH meter 700	25
<b>Figure 23</b>	Anton Paar Rheolab QC	26
<b>Figure 24</b>	Karl fisher 890 Titrando	26
<b>Figure 28</b>	METTLER TOLEDO T50 titrator	27
<b>Figure 29</b>	The set up apparatus of alumina and TEA reaction	27
<b>Figure 30</b>	Relation of viscosity and lap time when varied %TEA	31
<b>Figure 31</b>	Dipping study of slider bar in 85U8-6D lube from the old study	31
<b>Figure 32</b>	Record data shown in Tafel plot	32
<b>Figure 33</b>	Method to extrapolate Tafel plot	33
<b>Figure 34</b>	Raman spectra of alumina coated on AlTiC dipped at 100°C, 4 h.	35
<b>Figure 35</b>	Raman spectra of alumina and TEA reaction at 197°C, 2 h.	36
<b>Figure 36</b>	Raman spectra of solution after reaction (residue) at 197°C, 2 h.	37

<b>Figure</b>	<b>Page</b>
<b>Figure 37</b> NMR spectra (a) Solution before reaction, (b) Residue	38
<b>Figure 38</b> NMR spectrum of residue (Al-TEA complex) in range of 2-4 ppm	39
<b>Figure 39</b> Calculation ratio of EG and TEA before reaction	39
<b>Figure 40</b> Calculation ratio of EG and Al-TEA (after reaction)	41
<b>Figure 41</b> The proposed structure of Al-TEA complex from alumina (powder) reaction experiment.	41
<b>Figure 42</b> Optical microscope images of square coupon dipped sample at different conditions(5x)	42
<b>Figure 43</b> Optical microscope images of square coupon dipped samples at different conditions (20x)	43
<b>Figure 44</b> Optical microscope images of square coupon dipped samples at different conditions (50x)	44
<b>Figure 45</b> AFM images of square coupon dipped sample at different conditions	45





## Contents of tables

<b>Table</b>		<b>Page</b>
<b>Table 1</b>	Types of abrasive particles and their Mohs hardness values	9
<b>Table 2</b>	Advantages and limiting properties of synthetic base stocks	13
<b>Table 3</b>	Additives that function by physical interaction	14
<b>Table 4</b>	Additives that function by chemical interaction	14
<b>Table 5</b>	The percentage inhibition efficiency for corrosion of nickel in 1.0 M sulfuric acid	16
<b>Table 6</b>	The composition of lubricants in experiments	21
<b>Table 7</b>	The result of lapping experiment and viscosity measurement	29
<b>Table 8</b>	The results of dipping experiment	31
<b>Table 9</b>	Corrosion test with CoFe in lubricant containing different %TEA	32
<b>Table 10</b>	Water content for EG base lube with different condition	34
<b>Table 11</b>	pH and conductivity of each lube with different %TEA	34
<b>Table 12</b>	Viscosity of each lube with different %TEA	34
<b>Table 13</b>	TBN of lube with different %TEA	35
<b>Table 14</b>	Roughness test of dipping coupon in each lube	46



## Contents of appendix

Figure	Page
<b>Figure 1</b> Raman spectra of Ethylene glycol	52
<b>Figure 2</b> Raman spectra of Triethanolamine	52
<b>Figure 3</b> Raman spectra of solution before reaction (synthesis)	53
<b>Figure 4</b> Raman spectra of solution after reaction (residue)	53
<b>Figure 5</b> $^1\text{H-NMR}$ (400 MHz, $\text{CDCl}_3$ ) spectra of Ethylene glycol	54
<b>Figure 6</b> $^1\text{H-NMR}$ (400 MHz, $\text{CDCl}_3$ ) spectra of Triethanolamine	54
<b>Figure 7</b> $^1\text{H-NMR}$ (400 MHz, $\text{CDCl}_3$ ) spectra of solution before reaction (synthesis)	55
<b>Figure 8</b> $^1\text{H-NMR}$ (400 MHz, $\text{CDCl}_3$ ) spectra of solution after reaction (residue)	55



## List of abbreviations

nm	nanometer
°C	degree Celsius
%	percentage
mL	milliliter
kHz	kilohertz
kV	kilovolts
mm	millimeter
h	hour
mW	milliwatt
wt	weight
$R_a$	lowest height
$R_q$	average height
$R_{max}$	highest height
min	minute
$\mu\text{m}$	micron meter
$^1\text{H-NMR}$	proton nuclear magnetic resonance
s	singlet (NMR)
t	triplet (NMR)
b	broad (NMR)
Å	angstrom

ภาควิชาเคมี  
 คณะวิทยาศาสตร์  
 จุฬาลงกรณ์มหาวิทยาลัย

# Chapter1

## Introduction

### 1.1 Background

In the present, hard disk drive (HDD) is necessary devices for many organizations because of storing a lot of data. To store large amounts of data requires high quality hard disk drive to read and write data. A crucial function of hard disk drive is a storage data used by the file system and the computer operating system, and possibly inbuilt redundancy for error correction and recovery. Nowadays, the capacity of hard disk drive is up to 10 terabytes.

Slider heads is the most important component for reading and writing data process of hard disk drive. According to HDD industry, from all over production, the critical process in slider production is lapping process to obtain high quality slider head. Therefore, the development of lapping process has been studied. Lapping process directly affects the quality of slider heads by polishing slider's surface to reach specifications of thickness and electrical value of slider bar. Lapping process is divided into 2 processes that is rough lapping process and final lapping process using materials and any components; for example, lapping plate, diamond slurry and lubricant. The quality of slider head is measured in terms of electrical values; Electrical Lapping Guide (ELG) and Magneto Resistive Resistance (MRR). The other factor affecting on lapping process are roughness and lapping time. All factors described above indicate to quality of materials, machine and components to obtain requirement properties of slider head.

Industrial manufacturing lines must have production times cycle at least so that production can meet the customer demand. Lapping time also has impact on production times cycle. This factor can be affected by lapping pressure, plate rotation speed, abrasive grain size from slurry, lapping plate hardness and lubricant added during lapping process. The chemistry knowledge helpsto decrease lapping time in lapping process by adjusting the chemical composition in lubricant. The liquid lubricant used in lapping process is composes of ethylene glycol as base stock and many additives. Each additive has different function in lapping process. Triethanolamine, one of the additives, has been studied effect on lapping process because it helps reduce lapping time from Western digital Co,Ltd. experiments. This project studied effect of triethanolamine on lapping process by focusing on lapping time.

## 1.2 Theory

### 1.2.1 Hard disk drive

Hard disk drive is a part of computers that are used for writing and reading data. A hard disk drive has many elements such as slider, platters, spindle and actuator. The writing and reading element is slider head located at the end of a slider. The slider is a moving part above the platters in order to write and read data by using electrical current to generate magnetic field. In operation, the slider will perform reading and writing while flying above media at the height of 12 nm. To maintain this flying height across the different radius of the media, air bearing design, read and writer elements/slider bar will be lapped and polished to meet designed surface roughness, surface topography, as well as magnetic property. The slider surface roughness and texture are important factors in this application. **Figures 1** show schematic views of the slider-disk interface<sup>(1)</sup>.

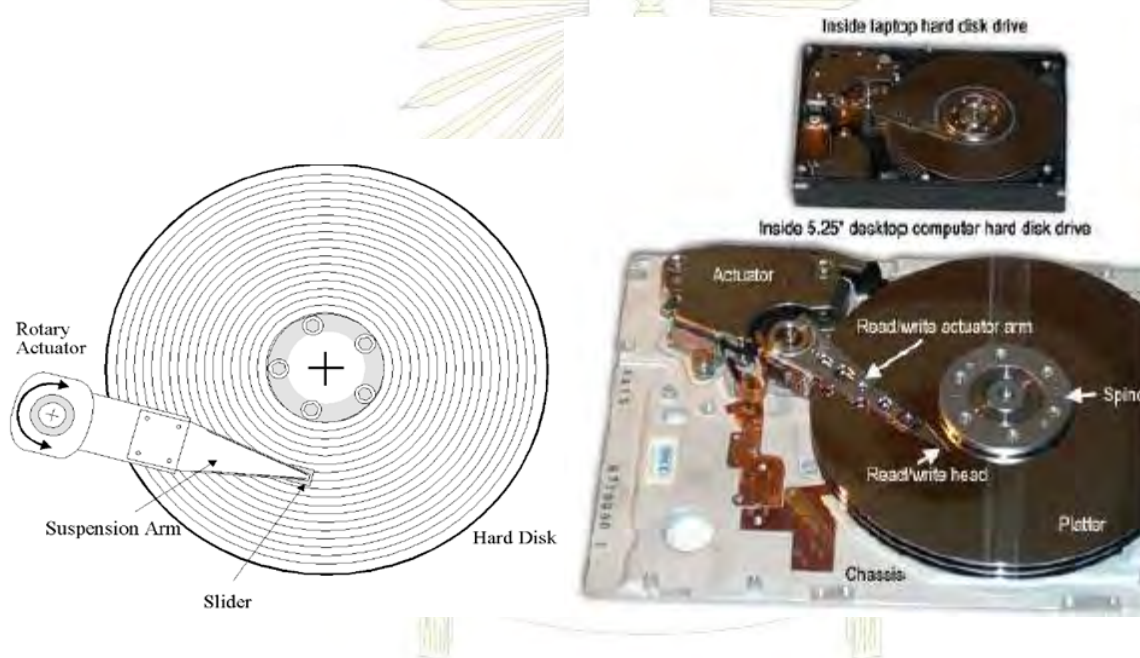


**Figure 1** Schematic views and real device of slider-disk interface.

### 1.2.2 Thin film recording head/slider bar manufacture

Thin film recording heads are manufactured as wafer (**Figure 2a**) in the first stage called wafer fabrication involving in deposition of head elements, photolithography, etching, electroplating and chemical-mechanical planarization. A single wafer containing 2000 head elements is cut in bar shape (**Figure 2b**) ready for lapping process. The chemical compositions of slider bars are comprised of 63% alumina ( $\text{Al}_2\text{O}_3$ ) which is a typical advanced ceramic material used for the wafer substrate, 36% Titanium carbide used for wear resistance and 1% deposited multilayers of thin film of metal-base alloys such as, Co-Fe, Ni-Fe and Ni-Mn which play important role in data processing of recording head. This material is called AlTiC substrate<sup>(2)</sup>. The brief production is shown in **Figure 3**.

The mixed material of AlTiC is pressed into square plates by simultaneous application of sintering technology (extreme pressure and heat in a hot press). The AlTiC substrate has an electrical conductivity property that is suitable for the data recording in the hard disk system application. After imported the substrates subjected to the additional processing, the small quantities of amorphous alumina are added over the AlTiC substrates models. Then the additional amorphous alumina is deposited by sputtering technique to form an insulation layer. Subsequently, micro-circuitry is deposited on the AlTiC substrates materials in order to create a flow path surface for electromagnetic conversion via processes of photolithography, which is the application of photoresist, exposing to light by a stepper to remove the surface materials by etching and also remove the photoresist layer. The surface of head facing the disk as the head flies is produced by lapping to reach there required transducer sensor target (sensor height) and good surface finish. The resulting micro-assemblies are further processed into recording heads to use as components for magnetic disk drives<sup>(3)</sup>.

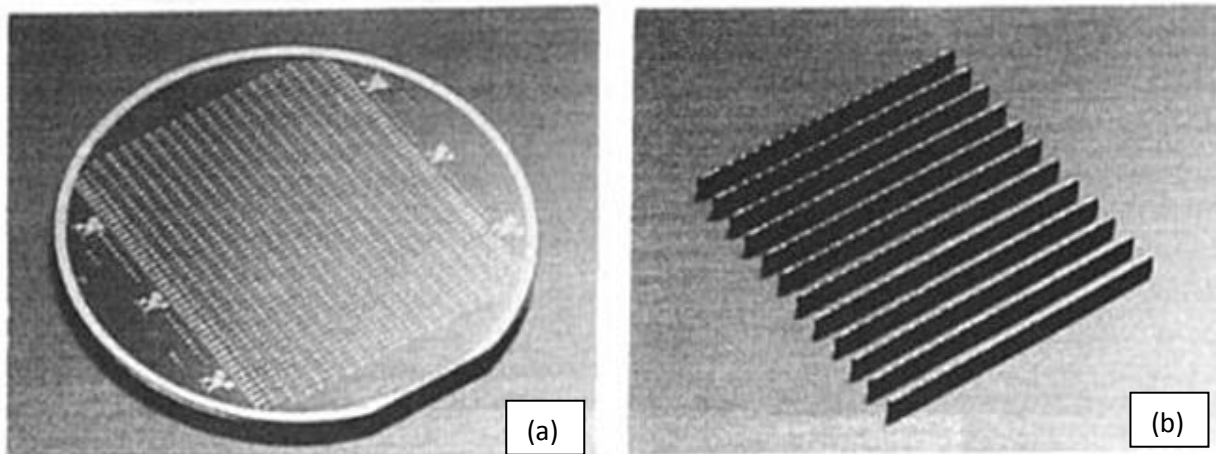


**Figure 2** Thin film head process. (a) Wafer (b) Slider bars

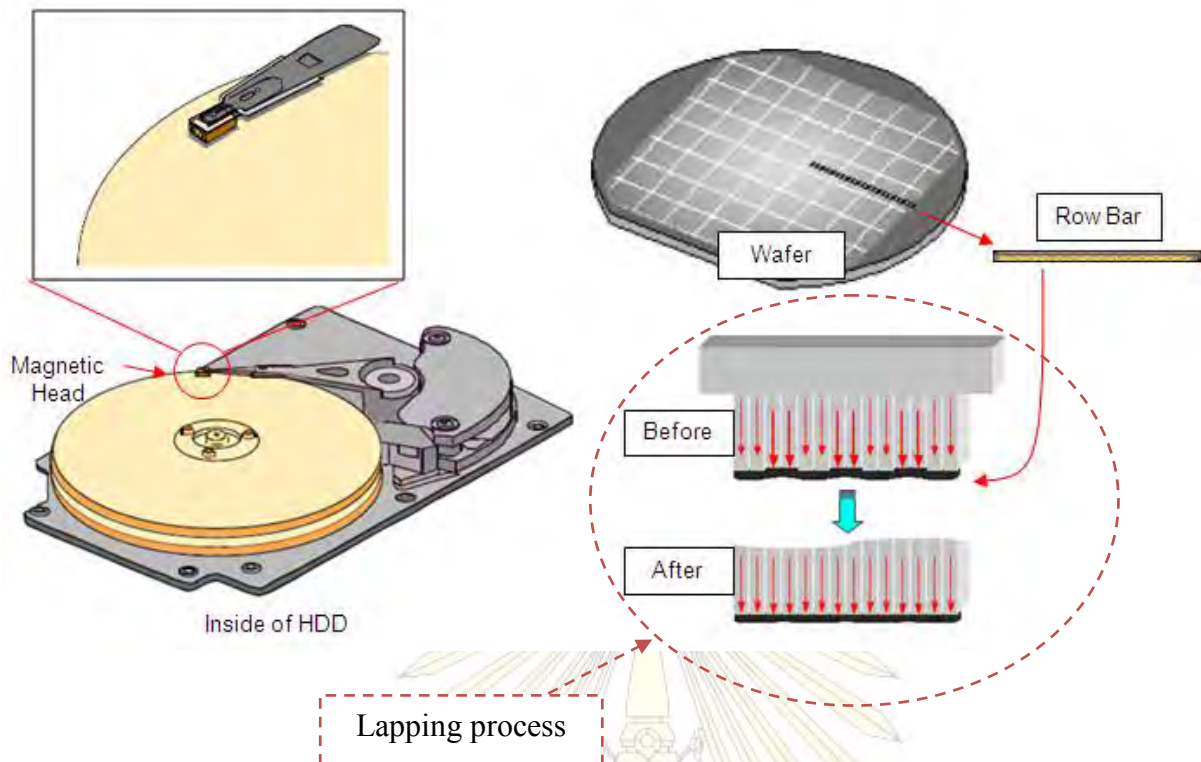


**Figure 3** Brief productions of thin film head.

### 1.2.3 Alumina

Aluminum is the metal which has been used worldwide in the technology industry for a long time. Since aluminum itself is very reactive to atmospheric oxygen so it can react spontaneously with oxygen and then forms thin film on the surface, which is called “Aluminum Oxide ( $\text{Al}_2\text{O}_3$ )” or “Alumina”. Alumina can be classified into 3 phases, which are crystalline, amorphous and liquid phases.

#### 1.2.3.1 Types of alumina

##### (a) Crystalline alumina

Alumina is most stable in crystalline phase known as  $\alpha$ -alumina, it is commonly referred to as corundum. It also exists in several polymorphs with a different number of transition alumina ( $\gamma$ ,  $\delta$ ,  $\kappa$ ,  $\chi$ ,  $\eta$  and  $\theta$  phases). These polymorphs are divided into two categories according to the structural arrangement of the oxygen atoms. Firstly, structures with FCC oxygen symmetries include  $\gamma$ ,  $\eta$  (cubic),  $\theta$  (monoclinic) and  $\delta$  (tetragonal or orthorhombic) phases. Secondly, structure is with oxygen based on HCP packing which represented by  $\alpha$  (trigonal), (orthorhombic), and  $\chi$  (hexagonal) phases. This is a review of its crystalline structure of alumina<sup>(4)</sup>.

A ceramic wafer of crystalline alumina and titanium carbide was used as head substrate, which was chosen because it satisfied all of the required specifications such as hardness, bending strength, specific resistance, thermal conductivity and optical constant and also good durability in start-stop operation. The microstructure of AlTiC is shown in **Figure 4**<sup>(5)</sup>.

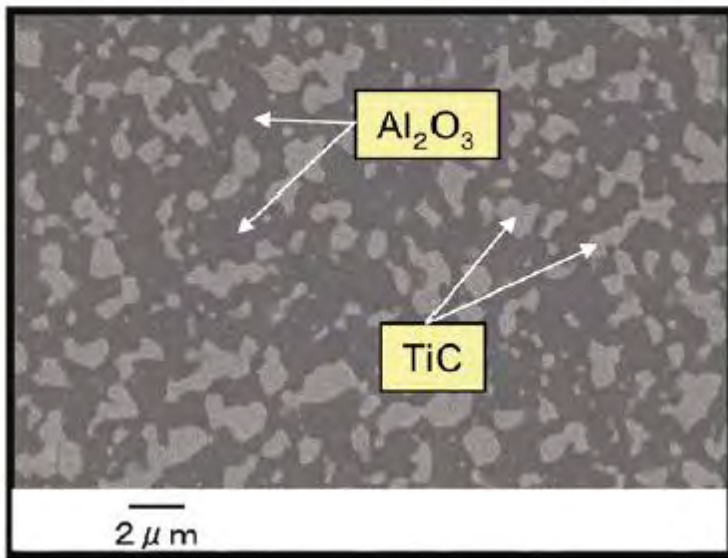


**Figure 4** Microstructure of TiC (gray) is dispersed in the Al<sub>2</sub>O<sub>3</sub> matrix (black).

#### (b) Amorphous alumina

The exact chemical properties and characteristics of amorphous alumina still cannot be evidently identified due to the random arrangement of amorphous phase structure. In comparison, crystalline alumina and amorphous alumina, the amorphous one is more reactive and less corrosive in resistance. In term of its application, amorphous alumina is used as deposited thin film by sputtering deposition and patterning of the layer to provide smooth surface for further layer processing and to insulate the heads from the slightly conductive ceramic substrate due to its low chemical conductivity<sup>(6)</sup>.

#### 1.2.3.2 Comparison of crystalline and amorphous alumina

Sung Keun Lee from Seoul National University and his colleague (2009)<sup>(7)</sup> explained the different of crystalline and amorphous alumina as follow. In crystalline  $\alpha$ -Al<sub>2</sub>O<sub>3</sub>, each aluminum atom is bonded to six oxygen atoms. But in its glassy form, about 55% of the aluminum atoms are four-coordinated (bonding to four oxygen atoms), and 42% are five-coordinated. As the two-dimension Nuclear Magnetic Resonance (2D NMR) technique generally requires relatively large amounts of sample, they have never been processed on thin films this way. Lee was the first person who came up with new invented technique and he believes that the result from this method will have a potential for revolutionizing the structural study of thin films and the surfaces of amorphous materials.



The result revealed that after the sample had been heated to 800 °C, the five-coordinated aluminum atoms transformed into four- and six-coordinated centers, indicating that the sample had begun to crystallize. After heating to 1200 °C, only six-coordinated aluminum atoms remained, forming crystalline  $\alpha$ -Al<sub>2</sub>O<sub>3</sub>.

According to the result, it could be implied that it is possible that the amorphous Al<sub>2</sub>O<sub>3</sub> could be a more active catalyst than its crystalline form since five-coordinated aluminum may have stronger catalytic activity than four- and six-coordinated aluminum. However, the large number of five-coordinated aluminum atoms also suggests that there are many three-coordinated oxygen atoms in the structure. In addition, contradicting the traditional view that oxygen atoms should bond to just two other atoms so that could explain the chemical instability of amorphous alumina's structure. The model structures of amorphous and crystalline alumina are shown in **Figure 5**.

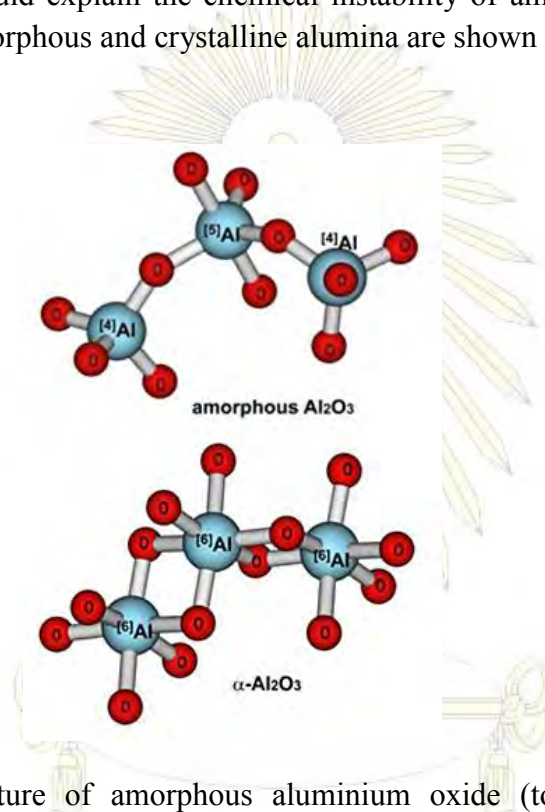


**Figure 5** Schematic structure of amorphous aluminium oxide (top) and crystalline  $\alpha$ -Al<sub>2</sub>O<sub>3</sub> (bottom)

ภาควิชาเคมี  
คณะวิทยาศาสตร์  
จุฬาลงกรณ์มหาวิทยาลัย

### 1.2.4 Lapping process

Lapping is used for several working materials which include glass, ceramic, plastic, metals and their alloys, sintered materials, satellite, ferrite, copper, cast iron, steel. Lapping is highly crucial techniques in hard disk production, read or write heads, semiconductor manufacturing. It has become a highly significant finishing method in ceramic seal industry. Lapping process is concerned with manufacturing techniques used for producing wanted surface of slider bar aspects with surface generation of adequate rate. The mechanics of lapping processes is carried out to produce flat surfaces. Workpieces are put in contact with a rotating plate and rotated in mechanical and frictional way in various motions which is done on lapping machine. The schematics of lapping composition are shown in **Figure 6**. According to HDD production, lapping is the process to remove material of slider bar by orientated lubricant and abrasive particles such as, diamond particles and alumina particles in form of liquid carrier which is applied to lapping plate or adding during lapping in order to obtain fine surface finish, high dimensional accuracy and flatness and lowest surface damage. An accurate perception of the interplay of factors in lapping plays a part in overcoming any problems in lapping process by optimizing the parameters and improving the quality of lapping. Lapping process has a numerous parameters that can be diverse so as to obtain the desired process output. The factors influencing lapping process are load, rotation of the lapping plate, material of the lapping plate, lapping time, kind of slurry used, grain size of the abrasive, flow rate and slurry concentration<sup>(8)</sup>.

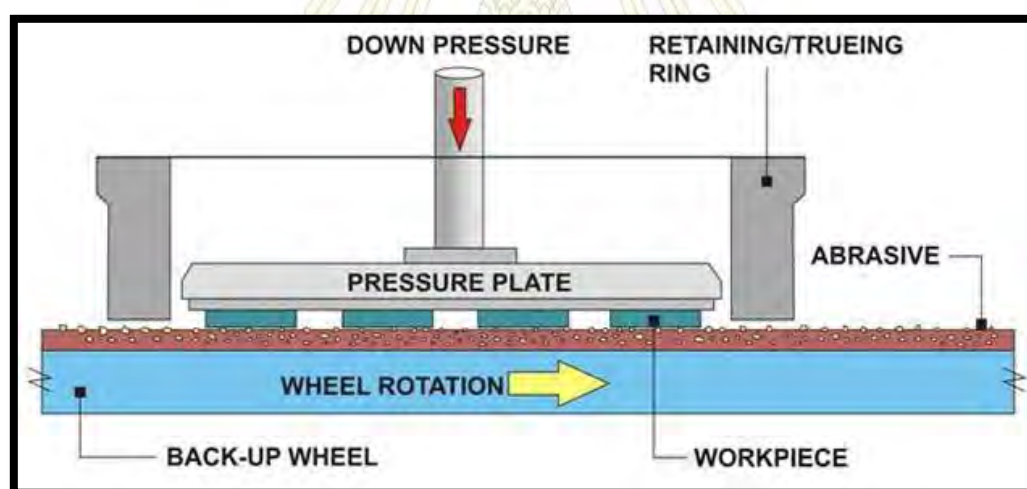


**Figure 6** Schematics of lapping composition.

The key factors affecting the lapping aspects are the type of the lapping plate, the type and size of the abrasive grains, and the type of the lapping fluid as follow

### 1.2.4.1 Lapping plate

The material of the lapping plate (**Figure 7**) is important because it is possible that a workpiece is badly scratched and contaminated with abrasives if the lapping plate is too hard. The composition of the lapping plate is of primordial importance as it can influence the results of the lapping process. A hard lapping plate resists being fixed firmly and deeply with abrasive particles. Therefore, a softer lapping plate allows abrasives to partially embed themselves in the lapping plate, leading to more sliding motion and material removal by ploughing. A wide variety of lapping plates is accessible for nearly any application<sup>(9)</sup>.



**Figure 7** lapping plates.

### 1.2.4.2 Abrasive

There are various abrasives that can be used for lapping: aluminum oxide (for general lapping with low surface roughness), silicon carbide (fast stock removal for hard or soft materials), boron carbide (for use with ceramic, carbide, and other hard materials), calcined alumina (for use with metals, optics, silicon wafers, and other semiconductor materials), diamond slurries and pastes (available in a vast variety of micron sizes and concentrations). The most extensively used abrasives in lapping process are the following<sup>(9)</sup>.

(a) Diamond is a sharpest and hardest abrasive. It is both a natural and human-made synthetic abrasive that gauges 10.0 on the Mohs scale of hardness (**Table 1**). So, it is the hardest material. Diamond is to the greatest degree suited for tungsten carbide and other so hard materials. When a plate is fixed deeply and firmly with the diamond abrasive, it cuts rapidly and gives fine finishes.

(b) Silicon carbide (SiC) is a fused, hard crystalline abrasive, 9.5 on Mohs scale. The achievement of fast cutting is with good crystal breakdown so as to maintain abrasive sharpness when being used for lapping either high or low tensile strength materials.

(c) Aluminum oxide ( $\text{Al}_2\text{O}_3$ ) is a fused abrasive with a very hard crystal structure which is hard to fracture. Its utilization is for lapping high tensile strength materials, rough lapping operations in which pressure can be applied to break down the crystals.

**Table 1** Types of abrasive particles and their Mohs hardness values

Abrasive	Mohs scale
Diamond	10.0
Cubic boron nitride	9.9
Silicon carbide	9.5
Aluminum oxide	9.0
38 White aluminum oxide	9.0
Corundum	9.0
Chromium oxide	8.5
Garnet	8-9.0
Quartz	7.0
Alumina (hydrates)	5-7.0

### Mechanisms of abrasive wear (**Figure 8**)

Wear is removal of the material from the surface of a solid body when subjected to contact and relative motion with another body. Abrasive wear occurs when a harder material is rubbing against a softer material<sup>(10)</sup>.

- If there are only two rubbing parts involved in the friction process the wear is called **two body wear**. In this case the wear of the softer material is caused by the asperities on the harder surface.
- If the wear is caused by a hard particle trapped between the rubbing surfaces it is called **three body wear**. The particle may be either free or partially embedded into one of the mating materials.

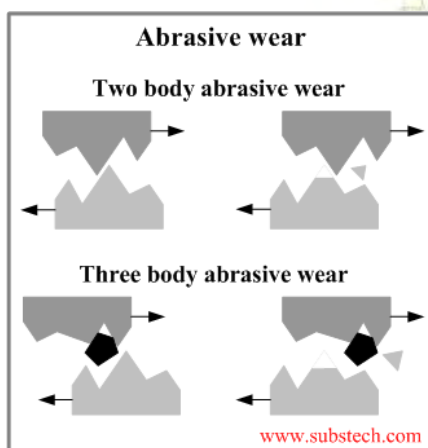


**Figure 8** Mechanisms of abrasive wear.

### 1.2.4.3 Lapping fluid and lubricant

Abrasive grains (**Figure 9a**) are carried to the lapping zone suspended in an oil or aqueous medium with the purpose of achieving a continuous and even distribution across the lapping plate. The availability of liquid carrier is in different viscosities to cover nearly any process requirement. Lubricants (**Figure 9b**) are required to reduce friction between the abrasive and the workpiece, minimize wear, transport debris and scattered fragment away from interface and provide cooling to diminish generated heat during lapping<sup>(9)</sup>.

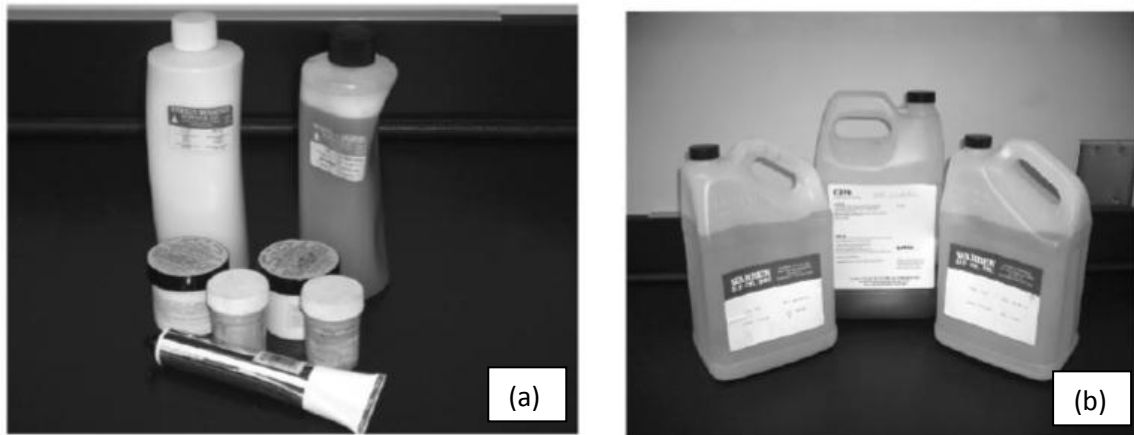


**Figure 9** (a) Abrasives and diamond slurry (b) lubricants

### 1.2.5 Lubricant in term of tribology

Tribology is the science focusing on the friction, wear and lubricant of the interaction between the surfaces that are associated with the motion. Lubricants refer to the materials used for the purpose of diminishing friction and wear between interacting surfaces during lapping to help tools and machines work effectively. The secondary objective is to help in cooling and washing impurities away from the contacting surfaces.

Lubrication can be classified into three main categories; hydrodynamic lubrication, boundary lubrication, and elasto-hydrodynamic lubrication<sup>(8)</sup>.

(a) Hydrodynamic lubrication (**Figure 10**) refers to the behavior of lubrication with oil film flowing between the contacting surfaces and separating the contacting surfaces definitely. Hydrodynamic lubrication works when the surface of one object begins to move past the surface of another object, the surfaces of the objects will face the oil. Since the oil has some viscosity, which gives resistance to the flow, it will not be possible for the objects to push all the oil out of the interface. However, a thin layer of oil will remain at the interface, making it possible for one surface to lift away from the other surface to a certain extent. When the objects move faster, the oil will move into the interface more, raising the other surface higher up until it is balanced. This means that the amount of the oil flowing into the interface is equal to the amount of the oil running out of the interface, and the interface thickness will be stable. The oil film in the interface must support the applied pressure, which is the weight of object that is lifted up. This oil film is maintained only when the objects move all the time.

### Full Fluid Film (Hydrodynamic) Lubrication

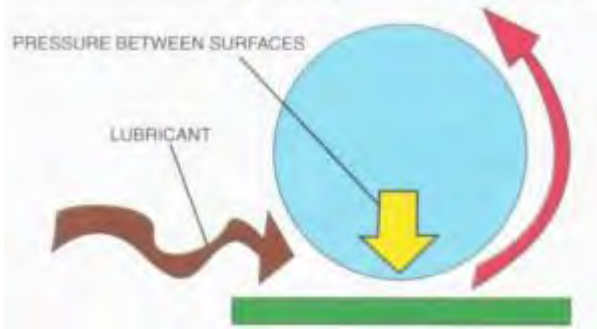


**Figure 10** Hydrodynamic lubrication diagram.

(b) Boundary lubrication (**Figure 11**) is the lubrication in which the oil film cannot be fully formed and completely separate the contacting surfaces. Also, the contacts between the peaks of the two contacting surfaces are inevitable as a result of the factors causing hydrodynamic lubrication is incomplete.

### Boundary Lubrication

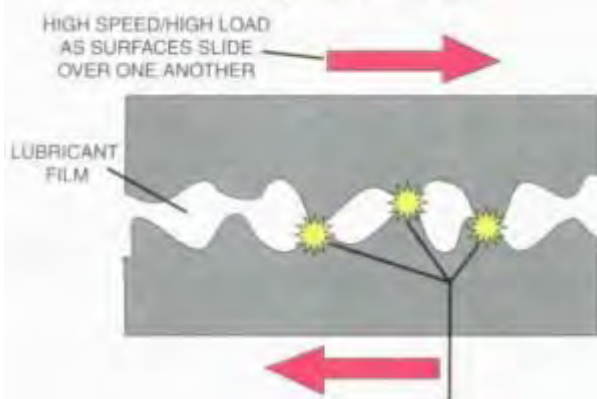


**Figure 11** Boundary lubrication diagram.

(c) Elastohydrodynamic lubrication (**Figure 12**) refers the behavior that the contacting surfaces temporarily collapse because of the extremely high pressure applied to small areas. The collapse makes the areas carrying the load expand. Also, with the increase in the viscosity of the lubricant under the high pressure, the lubrication film can completely separate the contacting surfaces.

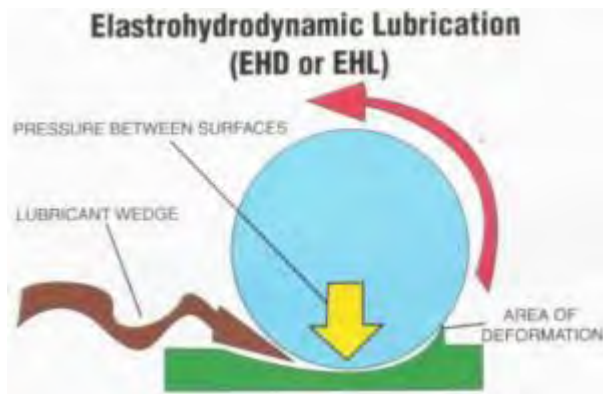


**Figure 12**Elasto-hydrodynamic diagram

### 1.2.6 Lubricants in term of chemistry

Modern high performing commercial lubricants are usually complex materials composed of a lubricant base stock formulated with an additive package for specific property enhancement of the resulting full lubricant formulation. Traditional lubricant systems are highly diverse, ranging mainly from common lube oils (non-aqueous liquids) to oil-in-water emulsions (used in water-miscible cutting fluids), water-in-oil emulsions (as in metal-forming), oil-in-oil emulsions (applied in metalworking), water-based solutions (applied in chip-forming metalworking operations), greases and pastes, and solid lubricants.

Water is a truly green lubricant or lubricant component. Water-based lubricants possess distinctive advantages over oil based lubricants (such as environmental compatibility, biocompatibility, availability, cost effectiveness). Their environmental compatibility makes them suitable for a number of industrial applications, such as food processing or textile and pharmaceutical manufacturing, where the use of oil-based lubricants can be problematic due to contamination issues. Base lubricants can be divided in 3 groups using lube sources<sup>(12)</sup>.

#### 1.2.6.1 Petroleum Base Lubricants (Mineral oils)

More than 90% of the lubricant market is dominated by mineral and related oils, which are heavily contaminating the environment, but have a wide availability and low price. The process of converting crude oil into finished mineral base oil is called refining. Base oils obtained by processing of crude petroleum are classified as refined and residual compounded. Mineral oils are complex mixtures of thousands of different compounds with a wide molecular weight distribution, but mainly  $C_{20}$  -  $C_{50}$  hydrocarbons including paraffins oil, naphthenic oil and aromatic oil<sup>(13)</sup>.

#### 1.2.6.2 Synthetic Base Lubricants

The production of synthetic lubricants starts with synthetic base stocks that are often manufactured from petroleum. The base fluids are made by chemically combining (synthesizing) low molecular weight compounds that have adequate viscosity for use as lubricants<sup>(14)</sup>. The primary performance advantage of synthetic lubricants is the extended service life capability and handling a wider range of application temperatures<sup>(15)</sup>. Other advantages, as well as limiting properties, are outlined in **Table 2**

**Table 2** Advantages and Limiting Properties of Synthetic Base Stocks

Synthetic	Advantages vs. mineral oil	Limiting properties	Example
Synthesized hydrocarbon Fluids (SHFs)	<ul style="list-style-type: none"> <li>• High temperature stability</li> <li>• Long life</li> <li>• Low temperature fluidity</li> <li>• Improved wear protection</li> <li>• Low volatility, oil economy</li> <li>• No wax</li> </ul>	<ul style="list-style-type: none"> <li>• Solvency/detergency</li> <li>• Seal compatibility</li> </ul>	<ul style="list-style-type: none"> <li>• Polyalphaolefins</li> <li>• Alkylated aromatics</li> <li>• Polybutenes</li> <li>• Cycloaliphatics</li> </ul>
Organic ester	<ul style="list-style-type: none"> <li>• High temperature stability</li> <li>• Long life</li> <li>• Low temperature fluidity</li> <li>• Solvency/detergency</li> </ul>	<ul style="list-style-type: none"> <li>• Seal compatibility</li> <li>• Mineral oil compatibility</li> <li>• Anti-rust</li> <li>• Anti-wear and extreme pressure</li> <li>• Hydrolytic stability</li> </ul>	<ul style="list-style-type: none"> <li>• Dibasic acid ester</li> <li>• Polyol ester</li> </ul>
Phosphate ester	<ul style="list-style-type: none"> <li>• Fire resistance</li> <li>• Lubricating ability</li> </ul>	<ul style="list-style-type: none"> <li>• Seal compatibility</li> <li>• Low viscosity index</li> <li>• Metal corrosion</li> <li>• Hydrolytic stability</li> </ul>	<ul style="list-style-type: none"> <li>• Triaryl phosphate ester</li> <li>• Triakyl phosphate ester</li> <li>• Mixed alkylaryl phosphate esters</li> </ul>
Polyglycols	<ul style="list-style-type: none"> <li>• Water versatility</li> <li>• High viscosity index</li> <li>• Low temperature fluidity</li> <li>• Anti-rust</li> <li>• No wax</li> </ul>	<ul style="list-style-type: none"> <li>• Mineral oil compatibility</li> <li>• Oxidation stability</li> </ul>	<ul style="list-style-type: none"> <li>• Polyalkylene</li> <li>• Polyoxyakylene</li> <li>• Polyethers</li> <li>• Glycol <ul style="list-style-type: none"> <li>✓ polyglycol esters,</li> <li>✓ polyalkylene glycol ester,</li> <li>✓ polyethylene glycol</li> </ul> </li> </ul>

### 1.2.6.3 Environmental lubricants

Environmental lubricants are fatty substances derived from animals, plants and fish. Vegetable oils provide another large source of lubricants. Fixed oils are generally composed of fatty acids and alcohols, the radicals of which are joined to form fatty acid esters<sup>(16)</sup>. The main characteristics of vegetable-based base oils (mainly C<sub>8</sub> to C<sub>24</sub>) are good boundary lubrication, wear protection, high flash point and low volatility. As to their tribological properties it appears that oils with longer carbon chains show lower friction and lower wear than shorter ones; saturated oils exhibit improved oxidative stability in high temperature and pressure applications<sup>(16)</sup>.



### 1.2.7 Additives

Additives are chemical compounds added to lubricating oils to impart specific properties to the finished in order to improve the performance characteristics of lubricating oils for suitable applications. Today, practically all types of lubricating oil contain at least one additive, and some oils contain additives of several different types. The amount of additive used varies from 5% to 30% of base oil. It is appropriate to consider additives types in term of how they function as part of the formulated oil, that is, physical interaction or chemical interaction shown in **Table 3 and 4**<sup>(17)</sup>.

**Table 3** Additives that function by physical interaction

Additive	Function
Antifoam	Prevents the formation of stable foam
Antimisting	Reduces the tendency to mist or aerosol
Color stabilizer	Slows darkening of fluids
Demulsifier	Enhances the separation of water and oil by promoting drop-coalescence and gravity-induced phase separation
Dyes	Impart color, mask color, product identification
Emulsifier	Reduces interfacial tension and allows dispersion of water
Friction modifier	Associate with the metal surface and improve sliding between surface
Odor control	Prevent or mask undesirable odors or maintain odor level
Pour point depressant	Lowers low-temperature fluidity by reducing the formation of wax crystals
Tackiness	Improve cohesion of fluid and nondrip quality
Thickener, solid filler	Converts oil into solid or semi-solid lubricant
VII	Improve viscosity-temperature characteristic
Water repellent	Impart water resistance to greases and other lubricants

**Table 4** Additives that function by chemical interaction

Additive	Function
Anti-bacteria (biocides)	Prevents or slow growth of bacteria in system
Anticorrosion (corrosion inhibitor)	Protects surface against chemical attack
Antioxidant	Reduces the rate of lubricant oxidation and deterioration and increases oil and machine life
AW	Reduces thin-film, boundary wear
Basicity control	Neutralizes acids from oxidation process
Detergent	Maintains surface cleanliness
Dispersant	Suspends and disperses undesirable combustion, wear, and oxidation products
EP (temperature)	Prevent seizing and increases load-carrying ability
Friction modifiers	Reduce friction and increase lubricity
Metal deactivator	Counteracts catalytic effects of surfaces by passivating surface

### 1.2.8 Ethylene glycol (EG) base stock

The lubricant used in lapping process is consisted of ethylene glycol as base stock and additives. Ethylene glycol is organic compound in group of polyglycols shown in **Figure 13**. They are the largest class of synthetic lubricant bases. Ethylene glycol is the most frequently used ingredient in coolants to minimize generated heat during lapping. The disadvantage of ethylene glycol is more corrosive than water, and more aggressive. On the other hand, one of the major advantages is that they decompose completely to volatile compounds under high temperature oxidizing condition. This results in low sludge buildup under moderate to high operating temperature or complete decomposition without leaving deposits in certain extremely hot applications. It has good viscosity-temperature characteristics, although at low temperature it tends to become somewhat more viscous than some of the other synthesized base. Moreover, pour point is relatively low, high temperature stability ranging from fair to good and may be improved with additives. Thermal conductivity is high. Not generally compatible with mineral oils or additives developed for use in mineral oils. Even if the glycol fluid does not initially contain any water, it has a tendency to absorb moisture from the air<sup>(18)</sup>.



**Figure 13** Structure of ethylene glycol.

### 1.2.9 Triethanolamine (TEA) additive in lubricant and literature review

Triethanolamine is a viscous organic compound that is both a tertiary amine and a triol shown in **Figure 14**. It is used in a number of industrial processes, and in the manufacture of a wide variety of consumer products. It is used to manufacture emulsifiers and dispersing agents for household detergents and polishes; lubricants, dyes and antistatic agents for textiles; agricultural herbicides; mineral and vegetable oils; paraffin and waxes; pharmaceutical ointments, and petroleum demulsifiers<sup>(19)</sup>.

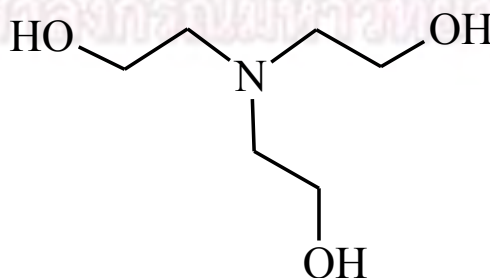


**Figure 14** Structure of Triethanolamine

### 1.3 Research Limitations

Triethanolamine, one of additives in ethylene glycol, is studied in this project. Because alumina ( $\text{Al}_2\text{O}_3$ ) and alloy are the components of slider bar, researcher will study chemical effect of TEA on alumina, CoFe as representative of metal-base-alloy and effect on lapping process. Lubricant has impact on several parameters in lapping process such as, lapping time, electrical value and surface morphology; but, in this project will focus on lapping time only.

### 1.4 Literature review

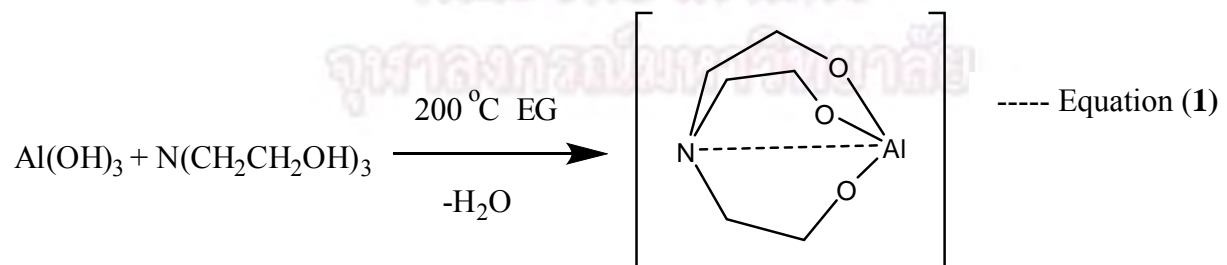
There are literature reviews of TEA reaction with aluminum oxide compound, metal and also using TEA in lapping as follow.

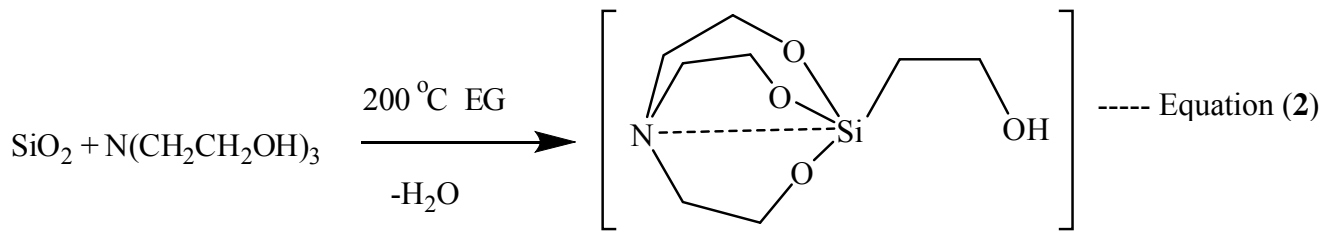
In 1985, V.S. Muralidharanand his team<sup>(20)</sup> studied 0.05M TEA as corrosion inhibitors for pure nickel in 1M sulfuric acid solutions by potentiostatic and adsorption study compared with 0.05M mono- and di- ethanolamine. The results from **Table 5** showed TEA exhibited lower inhibition than monoethanolamine and diethanolamine due to inductive effect, decreased the electron density on the nitrogen atom and steric effect. All of inhibitors obeyed Langmuir isotherm.

**Table 5** The percentage inhibition efficiency for corrosion of nickel in 1.0 M sulfuric acid

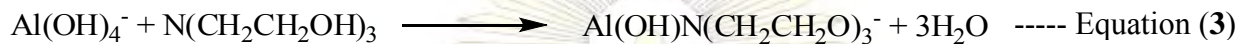
Solution	%Inhibition at 30 °C
1 M $\text{H}_2\text{SO}_4$	-
1 M $\text{H}_2\text{SO}_4$ + 0.05 MEA	73
1 M $\text{H}_2\text{SO}_4$ + 0.05 DEA	40
1 M $\text{H}_2\text{SO}_4$ + 0.05 TEA	33

In 2001, R. Baranwal and his team<sup>(21)</sup> studied TEA used as the reactant along with EG,  $\text{SiO}_2$  and aluminum hydroxide  $\text{Al}(\text{OH})_3$  to prepare the mullite precursor for mullite synthesized via equation (1) and (2) by Al-TEA and Si-TEA-EG complex formation. The mixture of 3 mole of TEA-Al and 1 mole of TEA-Si-EG was heated briefly in EG.





In 2004, D.A. Palmer and his team<sup>(22)</sup> studied the effect of additive TEA about the dissolution rate and equilibrium solubilities of Aluminum-Bearing Phases; such as, gibbsite, bayerite and boehmite. The results showed that TEA enhanced the dissolution of gibbsite  $\text{Al}(\text{OH})_3$  at  $90^\circ\text{C}$ . Moreover, Raman and NMR evidence suggested the existence of unique complexes between the aluminate anion and TEA following equation (3).



In 2013, H. Kim and his team<sup>(23)</sup> studied TEA used as a dispersant for the alumina slurry with different ratio to study the double sided lapping behavior of sapphire substrate containing alumina and Fe by using fixed diamond abrasive pad. The result shown in **Figure 15** when increased ratio of dispersant (TEA) per alumina slurry, the removal rate of lapping was raised because of the viscosity and alkaline pH of TEA.

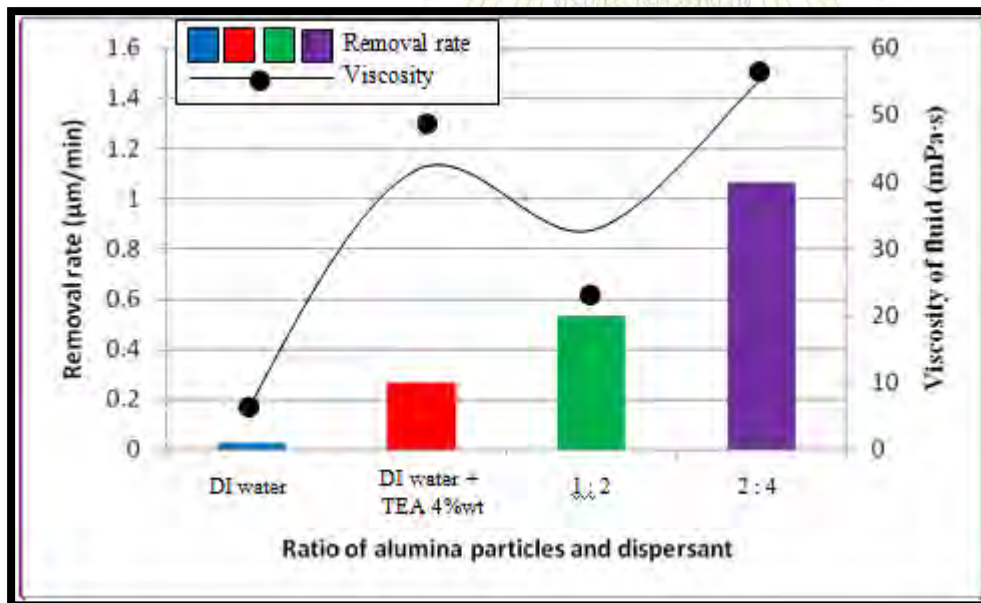


**Figure 15** Sapphire removal rate and viscosity as a function of particle to dispersant ratio (TEA).

## Objectives

1. Study on effect of %TEA on lapping time in final lapping process
2. Study on effect of %TEA on alumina and CoFe which is major and minor component in slider bar, respectively
3. Test physical properties in lubricant with different %TEA

## Expected benefits

1. Understand how TEA effect on lapping time in final lapping process
2. Suggest the suitable chemical components for future WD lapping solution



## Chapter 2

### Experimental

#### Equipment

- Round bottle flask
- Beaker
- Dropper
- Stirring rod
- Erlenmeyer flask
- Petri Dish
- Flat cell for corrosion test  
Platinum sheet, Ag/AgCl electrode
- Clamp
- Lapping plate
- Test tube
- Spatula
- Condenser
- Thermometer
- Heating mantle
- Heater and stirrer
- Inlet adapter
- Three way adapter
- Aluminum foil
- Rubber tube

#### Instruments

- Digital balance (Sartorius Basic, Scientific promotion Co.Ltd)
- Oven (MEMMERT UM500, BEC, Thailand)
- Nuclear Magnetic Resonance Spectrophotometer, NMR (YH 400 Bruker)
- ASL 200 fine lapping machine (supplied by Western Digital (Thailand) Co.Ltd)
- Potentiostat instrument (supplied by Western Digital (Thailand) Co.Ltd)
- pH and conductivity measurement (Eutech Instruments pH meter 700)
- Viscosity measurement (Anton Paar Rheolab QC)
- Water content measurement (Karl Fisher 890 Titrando)
- Total base number measurement (METTLER TOLEDO T50)
- Raman spectroscopy (Thermo Scientific DXR Raman Microscope)
- Optical microscope (Zeiss AxioCam HRc)
- Atomic force microscope, AFM (NovaScan)

#### Chemical substances

Chemical substance used as lubricant

- Ethylene glycol (Merck)
- Triethanolamine (supplied by Western Digital (Thailand) Co.Ltd)
- 85U8lubes (supplied by Western Digital (Thailand) Co.Ltd)

Chemical substance used in alumina reaction

- Hydrated aluminum oxide (Fluka)

Chemical used as NMR solvent

- $\text{CDCl}_3$  (Chloroform-d)

### Materials used as specimen

- Femto slider bar (strip)

Commercial slide heads made  $\text{Al}_2\text{O}_3\text{-TiC}$ (70%/30%) ceramic composites from Al of WesternDigital Company were used in this experiment. The slider heads with a flow path surface had a square shape of  $8.8 \text{ mm} \times 8.8 \text{ mm} \times 0.18 \mu\text{m}$  dimensions (width, length, and height) in row bar (**Figure16**), and were employed in dipping test. One slider bar contains the 52 individual slider heads and has the length of 460.75 mm. All the experiments using slider bars were carried out at room temperature ( $27^\circ\text{C}$ ).

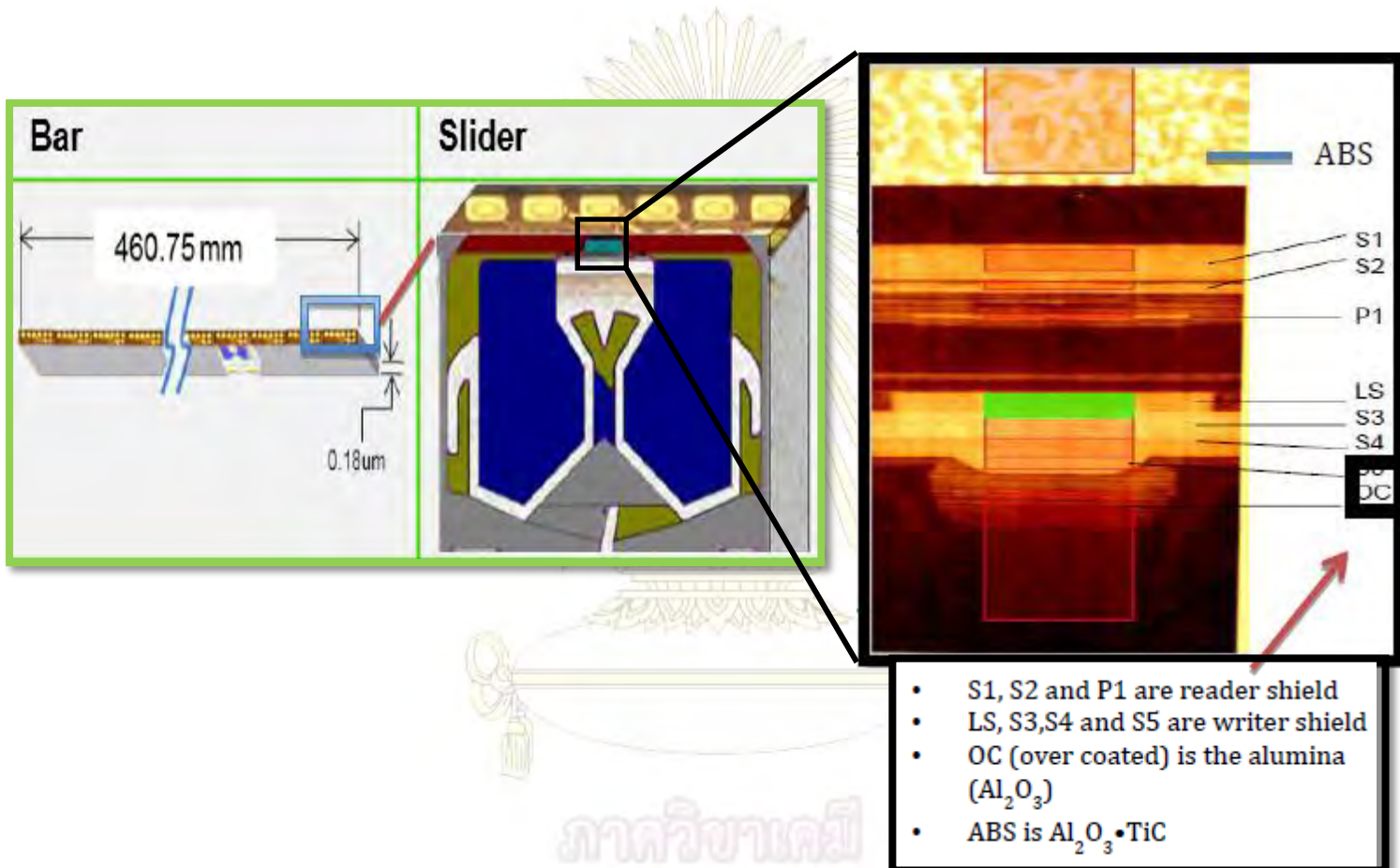


**Figure 16** Schematic of Slider head components

- Alumina coated on AlTiC coupon
- Co-Fe (70% Cobalt and 30% Iron) coated on Si substrate

### Technique used in experiment.

#### Potentiodynamic polarization

Potentiodynamic polarization techniques is used for study corrosion phenomena in term of electrochemical reaction; cathodic and anodic reactions. Corrosion reaction can be monitored at the surface of metal sample in the environment. The specimen potential ( $E_{corr}$ ) is scanned slowly in positive direction and therefore acts as an anode such that it corrodes.  $E_{corr}$  can be defined as the potential at which the rate of oxidation is exactly equal to the rate of reduction. The metal specimen is polarized in positive-going potential (anodic) and negative-going potential (cathodic) form  $E_{CORR}$  and the result is shown in graph called as Tafel plot. The corrosion current,  $i_{corr}$ , is obtained from a Tafel plot, and then substitute in equation (4) to obtain corrosion rate of metal<sup>(24)</sup>.

$$R_{corr} (P) = \frac{I_{corr}K}{dA} \quad \text{----- Equation (4)}$$

Where K is a constant equal to  $1.288 \times 10^5$  milli-inches per A per cm per year; EW is the equivalent weight of the specimen; d is the density ( $\text{g}\cdot\text{cm}^{-3}$ ) of the specimen; and A is the surface area ( $\text{cm}^2$ ) of the specimen.

The lubricants used in this project are in **Table 6**.

**Table 6** The composition of lubricants in experiments

no.	Lube solution code	Composition (wt.%)					
		TEA	Inhibitor A	Inhibitor B	Imidazole	EG base	Total
1	85U8	0.00	0.150	0.150	0.011	99.689	100.00
2	85U8-6	3.00	0.150	0.150	0.011	96.689	100.00
3	85U8-6A	6.00	0.150	0.150	0.011	93.689	100.00
4	85U8-6D	10.00	0.150	0.150	0.011	89.689	100.00
5	0%-TEA (Pure EG)	0.00	0.000	0.000	0.000	100.000	100.00
6	3%-TEA	3.00	0.000	0.000	0.000	97.000	100.00
7	6%-TEA	6.00	0.000	0.000	0.000	94.000	100.00
8	10%-TEA	10.00	0.000	0.000	0.000	90.000	100.00



## 2.1 Lapping experiments

Lapping experiments were performed on ASL 200 fine lap machine to lap femto slider bar (from relief cut with diamond wheel) with Sn-Bi 48-52% plate embedded with 70 nm. of diamond abrasive by adding different lube including, 85U8, 85U8-6, 85U8-6A and 85U8-6D, respectively. Before lapping, clean lapping plate with de-ionized water and wipe by tissue paper for plate recondition. The lapping condition is the same as industrial work to reach target resistance (R-ELG). Lapping time was obtained from machine. The material removal rate was calculated by using program from machine via R-ELG transfer to loss mass and the average value of R-ELG was reported together with standard deviation. The lapping experiment was done for 4 bars per one lubricant. Moreover, lapping experiment was done re-run for another plate. The components of lapping process are shown in **Figure 17**.

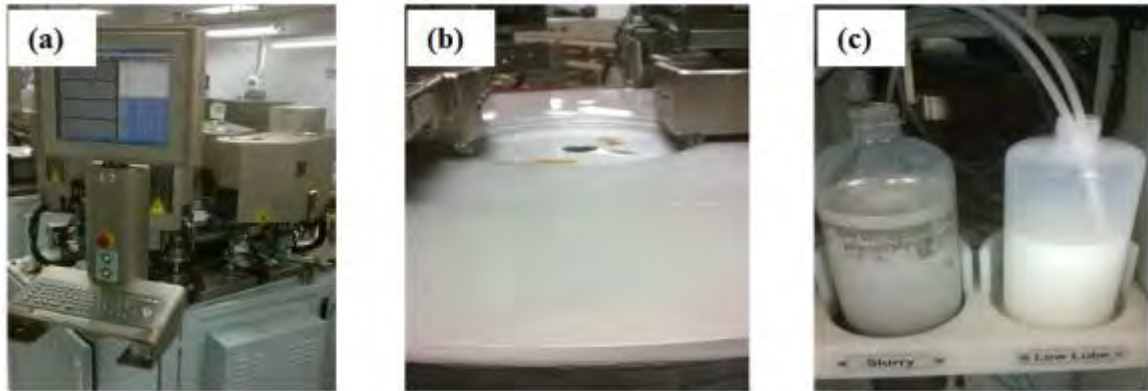


**Figure 17** Lapping components (a) ASL 200 fine lap machine  
(b) diamond particle embedded on Sn-Bi plate (c) Lubricant.

## 2.2 Dipping test

### 2.2.1 Slider bar (strip sample)

Dipping test is dip/soak slider bar into 100 mL of 0%-TEA, 3%-TEA, 6%-TEA and 10%-TEA in beakers at 23 °C for 3 days, another bar keep in system without lube at the same time to use as control bar. Before dipping, AFM need to be done to measure alumina recession and surface roughness before dipping compared to after dipping. When dipping finish, bars were taken it to AFM to measure alumina recession and analyze the surface roughness by focusing on overcoat area or alumina part in slider bar. The set up of experiment is shown in **Figure 18**.

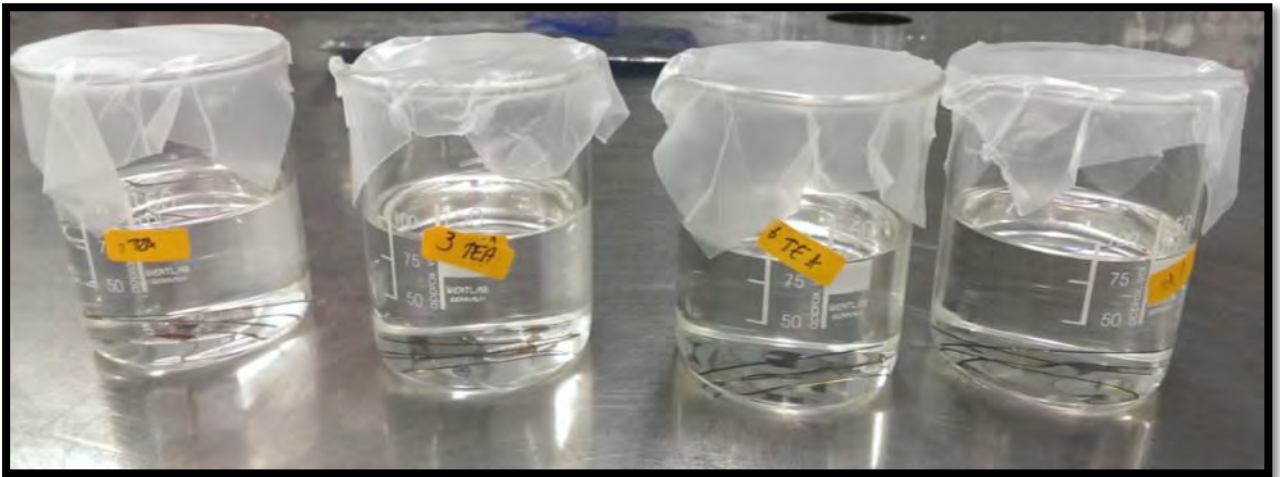


**Figure 18** Slider bars were dipping in prepared solutions

### 2.2.2 Square coupon dipping test

Dipping experiment was done by soaking the amorphous alumina coated on AlTiC substrate into 0%-TEA and 6%-TEA in beaker for 4 h. at 100°C and keep one coupon in close system to use as blank. The set up of experiment is shown in **Figure 19**.



**Figure 19** Coupon was dipping in prepared solutions

### 2.3 Corrosion test of CoFe with TEA concentration effect

The commercial CoFe (70% Cobalt and 30% Iron) coated on Si substrate is used in this study. The specimen was cut to 2 mm. x 3 mm. x 1 mm. coated with UV-photolysis and cleaned with iso-propyl alcohol before corrosion test. The exposed area of CoFe substrate is 1 mm<sup>2</sup> in electrochemical test as working electrode. Platinum sheet is used as counter electrode and Ag/AgCl (3M KCl) is used as reference electrode. Potentiostat technique was used for studying corrosion by using Autolab 1.9.16 software, the instrument was shown in **Figure 20**.

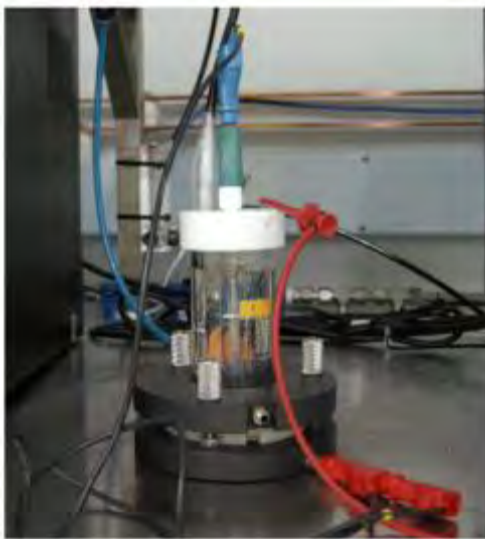


**Figure 20** Flatcell tool

The scan rate of the polarization curves was 0.002 V/s and the range of potential started from -0.6 V to 0.8 V. The experiment was done 3 times/lube. The schematic diagram of corrosion test tool is shown in **Figure 21**.

ภาควิชาเคมี  
คณะวิทยาศาสตร์  
จุฬาลงกรณ์มหาวิทยาลัย

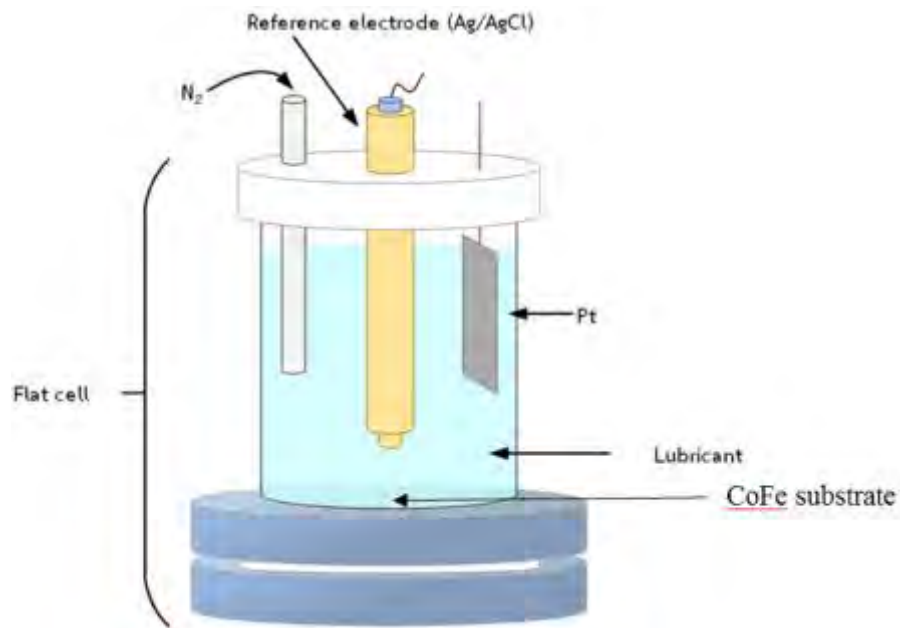


**Figure 21** Diagram of corrosion test tool

## 2.4 Physical and chemical properties measurement

### 2.4.1 pH and conductivity

The pH values were measured by METTLER TOLEDO tool using 30 mL of each lube (**Figure 22**).



**Figure 22** Eutech Instruments pH meter 700

### 2.4.2 Viscosity

The viscosity was measured by Anton Paar using 50 mL of each lube (**Figure 23**). The viscosity was measure on constant sheer rate mode.



**Figure 23** Anton Paar Rheolab QC

### 2.4.3 Water content

The water content was measured by Karl fisher instrument and used Karl fisher reagent (**Figure 24**). The amount of sample was 20 milliliters.



**Figure 24** Karl fisher 890 Titrand

#### 2.4.4 Total base number(TBN)

The total base number was measured by METTLER TOLEDO T50 titrator with DG116-Solvent probe (**Figure 28**). The amount of sample is 1 g.



**Figure 28** METTLER TOLEDO T50 titrator

#### 2.5 Alumina powder and TEA reaction

The reaction between alumina powder and TEA was done by placing 5.03 g (0.064 mmol) of  $\text{Al}_2\text{O}_3 \cdot 3\text{H}_2\text{O}$  (Fluka) into the 100mL rounded-bottle-flask and followed by adding the lube which contains 13.3 mL (0.100 mmol) of TEA and 30 ml (0.538mmol) of EG and then, stirred for 1 day. After that, carried on the distillation by heating the mixture at 197–205°C for around 1.30 h to reach boiling of EG by using heating mantle as well as covered the system with foil. Finally, filtrate remaining powder out and keep the residue solution in round bottle flask for characterization by Raman spectroscopy and NMR spectroscopy. The set up apparatus was shown in **Figure 29**.



**Figure 29** The set up apparatus of alumina and TEA reaction

## 2.6 Material Characterization

### 2.6.1 Square coupon

The dipped alumina coupon including with before and after dipping was characterized by Raman spectroscopy. In addition, coupon after dipping in 0%-TEA and 6%-TEA at 100°C for 4 h. were also observed by optical microscope, AFM and roughness test to observe the morphology of surface before compared to after dipping.

### 2.6.2 Solution before and after of alumina powder reaction

The solutions before and after reaction were characterized by Raman spectroscopy and NMR spectroscopy. The Raman measurement was carried out using Invia Reflex confocal Raman microprobe with Ar<sup>+</sup> laser of 514 nm in backscattering mode, with laser spot of 10 μm for surface analysis. An exposure time of 50s and 2 accumulations were used, with 50x objectives. The laser power was 25 mW. Raman spectra were collected on at least 3 representative spots from the sample surface. The spectra were observed to be reproducible.



## Chapter 3

### Result and discussion

#### 3.1 Lapping experiment

The lapping time as a function of %TEA and viscosity, the data is shown in **Table 7**. The target loss mass was fixed at 50 nm. According to the recession plot shown in **Figure 30** when %TEA increases, the lapping time will decrease quite linearly from 0%TEA to 6%TEA. From the **Table 7**, different value of lapping time from increasing 6% to 10% is lesser than 0% to 3% TEA and 3% to 6% TEA. However, in hard disk drive industry, around 2 minutes is acceptable. Material removal is caused from mechanical removal along with chemical removal.

**Table 7** The result of lapping experiment and viscosity measurement

Lube name	TEA (wt.%)	Viscosity (Pa•s)	Total lap time (min)
85U8	0	$2.622 \times 10^{-2}$	3.02
85U8-6	3	$2.723 \times 10^{-2}$	2.69
85U8-6A	6	$3.024 \times 10^{-2}$	2.27
85U8-6D	10	$3.303 \times 10^{-2}$	2.09

From the literature review, Hyuk-Min Kim and his team<sup>(23)</sup> performed lapping by using fixed-abrasive diamond pad and triethanolamine as dispersant to lap sapphire containing alumina as well as iron and they found lapping has to be performed with a high viscous slurry/fluid, as it involves high friction.

Therefore, the viscosity effects on the mechanical removal. The higher %TEA, the higher viscosity related to high friction contributing to reduce increase material removal rate or reduce lapping time, the trend showing in **Figure 30**.



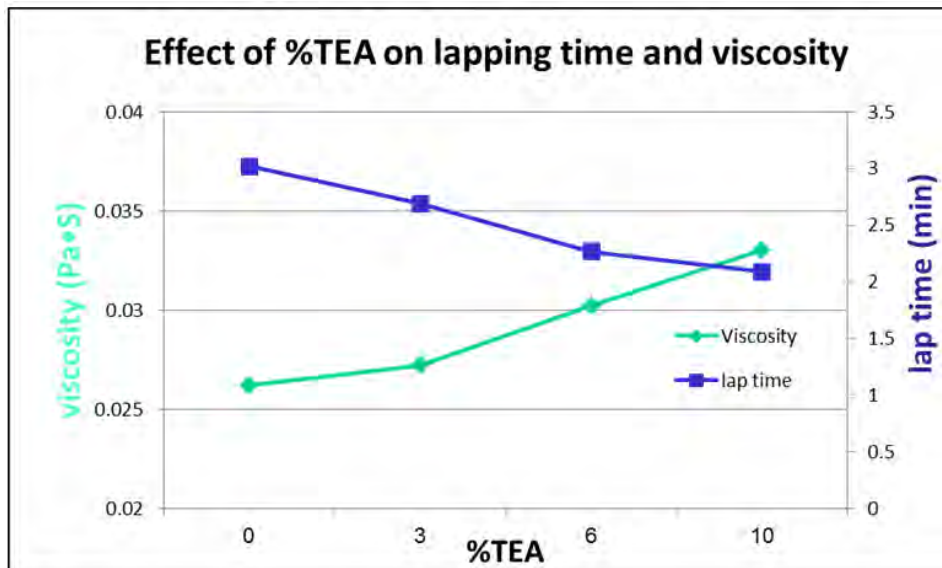


**Figure 30** Relation of viscosity and lap time when varied %TEA

Besides, the effect of chemical removal also effects on lapping process by reaction between alumina which is the major component in slider bar and triethanolamine. Thus, the chemical effect of triethanolamine was studied by dipping test.

### 3.2 Dipping test (Strip sample)

The chemical removal effect was studied by dipping test. According to previous study by Western digital, the result was shown in **Figure 31**, the overcoat or alumina part showed more recession than the other parts when dipping in lubricant containing 10%TEA in EG base with fixed amount of other additives (85U8-6D). So, this project also studied effect of TEA on alumina part in slider bar.

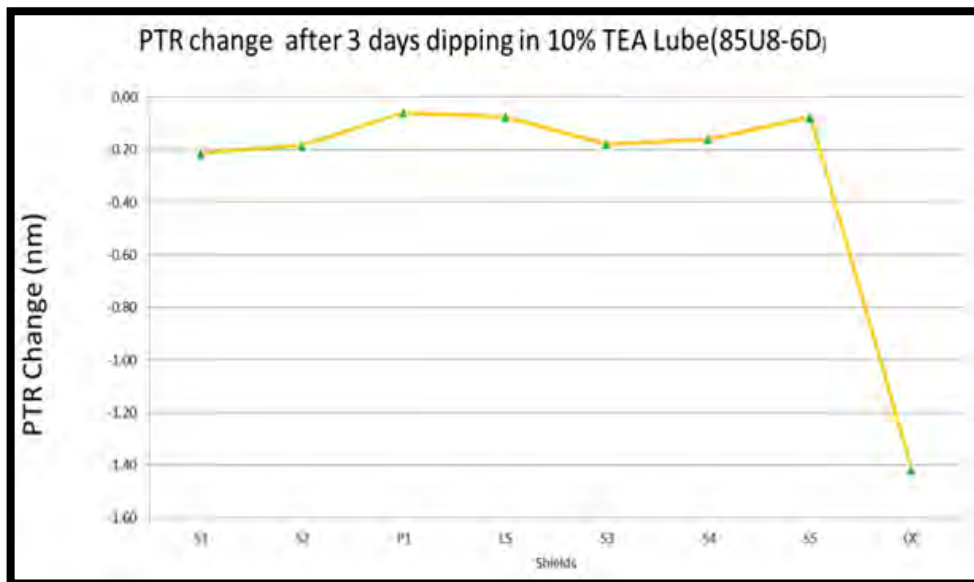


**Figure 31** Dipping study of slider bar in 85U8-6D lube

**Table 8** showed the results of dipping test. For dipping result showed the maximum %TEA effects on highest alumina recession is 6%TEA because at concentration 6%TEA in ethylene glycol is homogenized solution; while at 10%TEA bilayer solution was observed.

For 10%-TEA, the phase separation occurred because the intramolecular force of triethanolamine is stronger than intermolecular force between TEA and ethylene glycol. This results from the molecular dipole moment of two chemical substances are different causing the dissolution is quite poor ( $\mu_{EG} = 2.20^{(25)}$  and  $\mu_{TEA} = 3.48^{(26)}$ ).

**Table 8** The results of dipping experiment

Lubricant	Alumina recession (nm.)
No dipping	-0.470
0%-TEA	-0.475
3%-TEA	-1.616
6%-TEA	-2.617
10%-TEA	-1.201

### 3.3 Corrosion test of CoFe with TEA concentration effect

Analytical corrosion testing was carried on in order to measure corrosion potential ( $E_{\text{corr}}$ ) and corrosion current ( $i_{\text{corr}}$ ) to study corrosion rate and corrosion behavior of CoFe instead of alumina because the working electrode sample must be conducting material; however, CoFe is one of component in slider bar. It is a representative for this corrosion test. The result of each lubricant is shown in **Figure 32** and **Table 9**.

**Table 9** Corrosion test with CoFe in lubricant containing different %TEA.

Lubricant	$I_{\text{corr}}$ (nA)	$E_{\text{corr}}$ (V)	Corrosion rate (mm/year)	Corrosion rate ( $\text{\AA}/\text{min}$ )
0%TEA	66.173	-0.026	$0.769 \times 10^{-3}$	0.0146
3%TEA	101.638	-0.142	$1.181 \times 10^{-3}$	0.0224
6%TEA	206.343	-0.139	$2.398 \times 10^{-3}$	0.0456
10%TEA	208.950	-0.164	$2.428 \times 10^{-3}$	0.0462

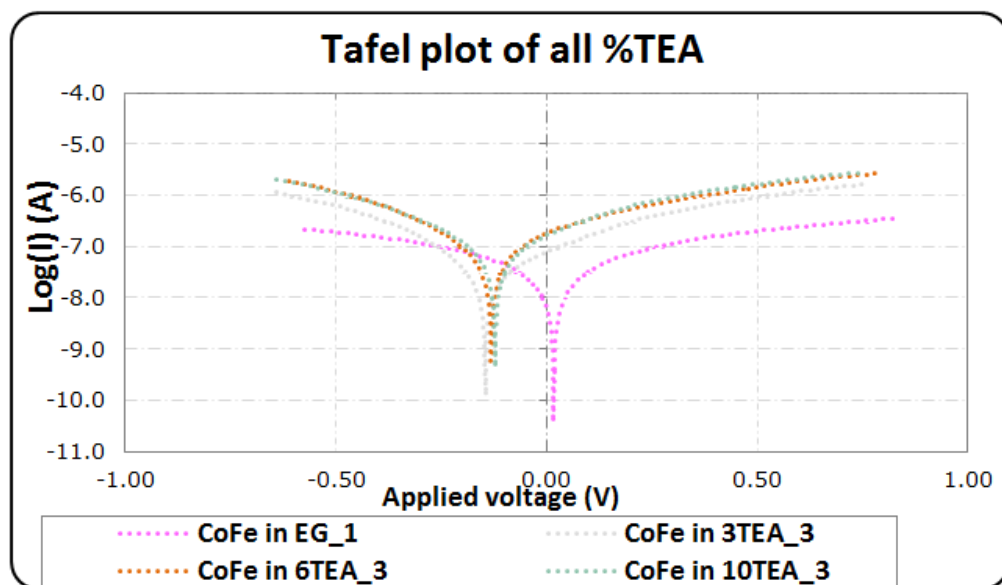


**Figure 32** Record data shown in Tafel plot

The result showed that CoFe substrate in lubricant containing TEA can corrode easier than without TEA because the applied potential to make corrosion is lower. From the Tafel plot, the extrapolation method is used for obtain corrosion current as shown in **Figure 33** and then substitute in equation<sup>(27)</sup>(4) to solve a corrosion rate as result in **Table 9**.

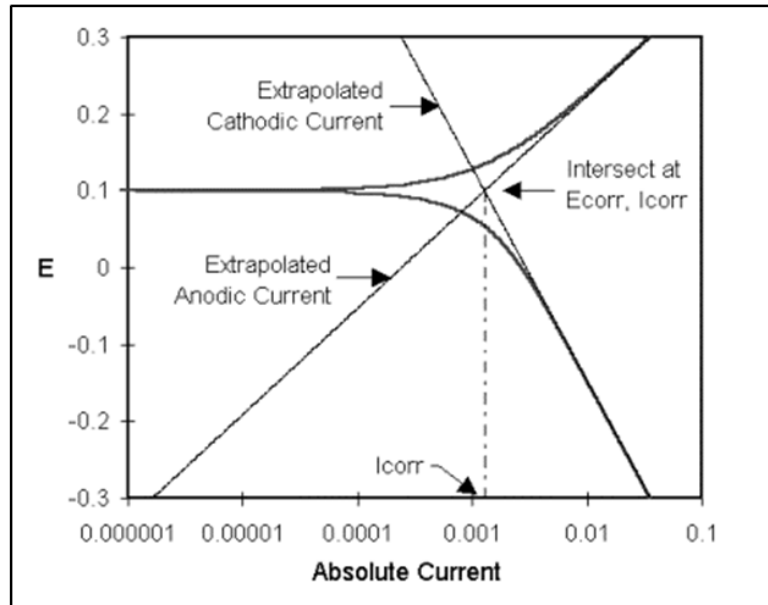


**Figure 33** Method to extrapolate Tafel plot

The Tafel plot is separated in two sides. The upper side is cathodic reaction of water molecule in lube since ethylene glycol can absorb the water from the air (**Table 10**) as well as the lower side is anodic reaction of cobalt and/or iron, which corroded in each lube with different %TEA. From the corrosion rate, when %TEA was increased from 0 to 6%wt., the corrosion current raised, contributing to increasing corrosion rate; however, when TEA increases from 6% to 10%, the corrosion rate slightly expanded. So, TEA promoted corrosion of Fe by complex formation<sup>(28)</sup>.

### 3.4 Physical and chemical properties measurement

#### 3.4.1 Water content

The water content results were shown in **Table 10**. Both ethylene glycol and triethanolamine can absorb water in the air, contributing to effect on the corrosion of metal by rising conductivity value<sup>(29)</sup>.

**Table 10** Water content for EG base lube with different condition

Lube/Solution	Water content (%weight)	
	1	2
Ethylene glycol (Fresh prepared)	0.1507	0.1503
Ethylene glycol (Left for 2 days)	28.2379	28.6944
6%-TEA (Left for 2 days)	32.6092	33.0868

### 3.4.2 pH and conductivity

**Table 11** showed pH and conductivity results. The amount of TEA effects on pH because TEA is basic property following Lewis-base theory. Also, effect to conductivity increased from an ionization of hydroxyl group in TEA molecule.

**Table 11** pH and conductivity of each lube with different %TEA

Lube	pH	Conductivity ( $\mu\text{S}/\text{cm}$ )
0% TEA	7.67	0.8
3% TEA	9.96	3.8
6% TEA	10.073	4.9
10% TEA	10.017	6.2

### 3.4.3 Viscosity

The viscosity results were showed in **Table 12**. The amount of TEA effects on viscosity because TEA is a viscous liquid (404 cP at 30°C)<sup>(19)</sup>.

**Table 12** Viscosity of each lube with different %TEA

Lubricant	Viscosity (Pa·s)
0%-TEA	$2.622 \times 10^{-2}$
3%-TEA	$2.723 \times 10^{-2}$
6%-TEA	$3.024 \times 10^{-2}$
10%-TEA	$3.303 \times 10^{-2}$

### 3.4.4 Total base number

Total base number (TBN) values of lubricant were shown in **Table 13**. When %TEA increases, TBN will increase since TEA is basic property due to amine base functional group.

**Table 13** TBN of lube with different %TEA

Lubricant	TBN
0%-TEA	-
3%-TEA	11.76
6%-TEA	25.10
10%-TEA	37.15

## 3.5 Characterization

### 3.5.1 Raman spectroscopy of dipping coupon

The Raman results of coupon dipped in 6%TEA because at this ratio provided highest alumina recession. The Raman spectra of coupon after dipping showed in **Figure 34**. It has the peak of TEA on  $\text{Al}_2\text{O}_3$  coated on AlTiC substrate at around  $1392\text{ cm}^{-1}$  which belongs to OH bending of TEA<sup>(30)</sup>. Hence, only TEA reacts with alumina and EG acted as solvent.

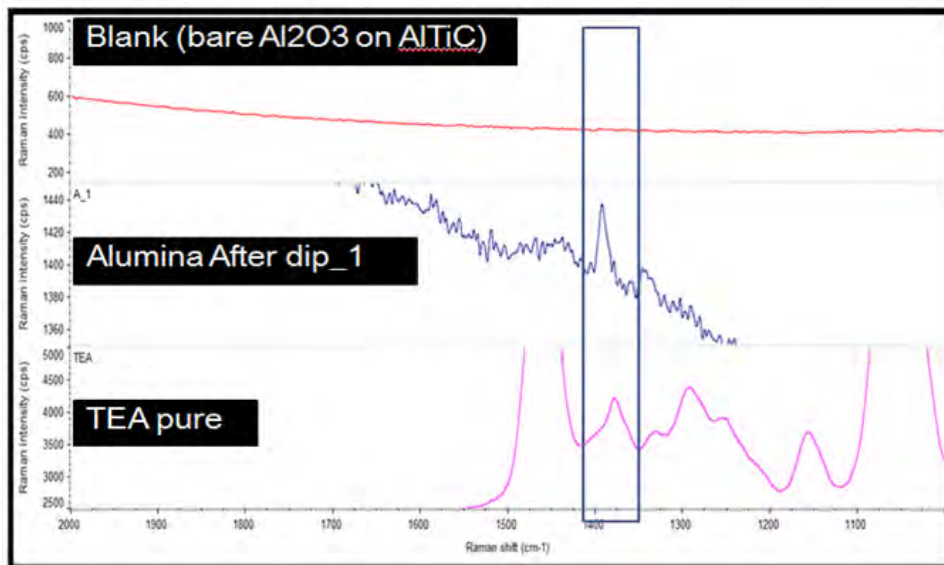


**Figure 34** Raman spectra of alumina coated on AlTiC dipped at  $100^\circ\text{C}$ , 4 h.

Solid powder alumina (Hydrated aluminum oxide) was selected to use instead of alumina coupon because the amount of alumina in coupon sample is too small to react with 6%-TEA and hard to characterize by Raman spectroscopy, NMR spectroscopy and ICP-MS.

### 3.5.2 Raman and NMR spectroscopy of solution of alumina reaction (alumina powder)

The Raman spectrum of alumina and TEA reaction showed in **Figure 35** and **36**. The Raman spectra of solution after reaction (residue) showed new peak at  $1159\text{ cm}^{-1}$  compared to solution before reaction (Synthesis) which identified as C-O and C-N stretching<sup>(31),(32)</sup> of Al-TEA complex, which related to our intermediate chemical in suggested mechanism (**Figure 41**). The identified functional groups of other peaks of residue showed in **Figure 36**. Moreover, the peak area at  $1091\text{ cm}^{-1}$ , which identifies as OH bending decrease since some of TEA reacts with alumina as well as evaporation of EG<sup>(33)</sup>.

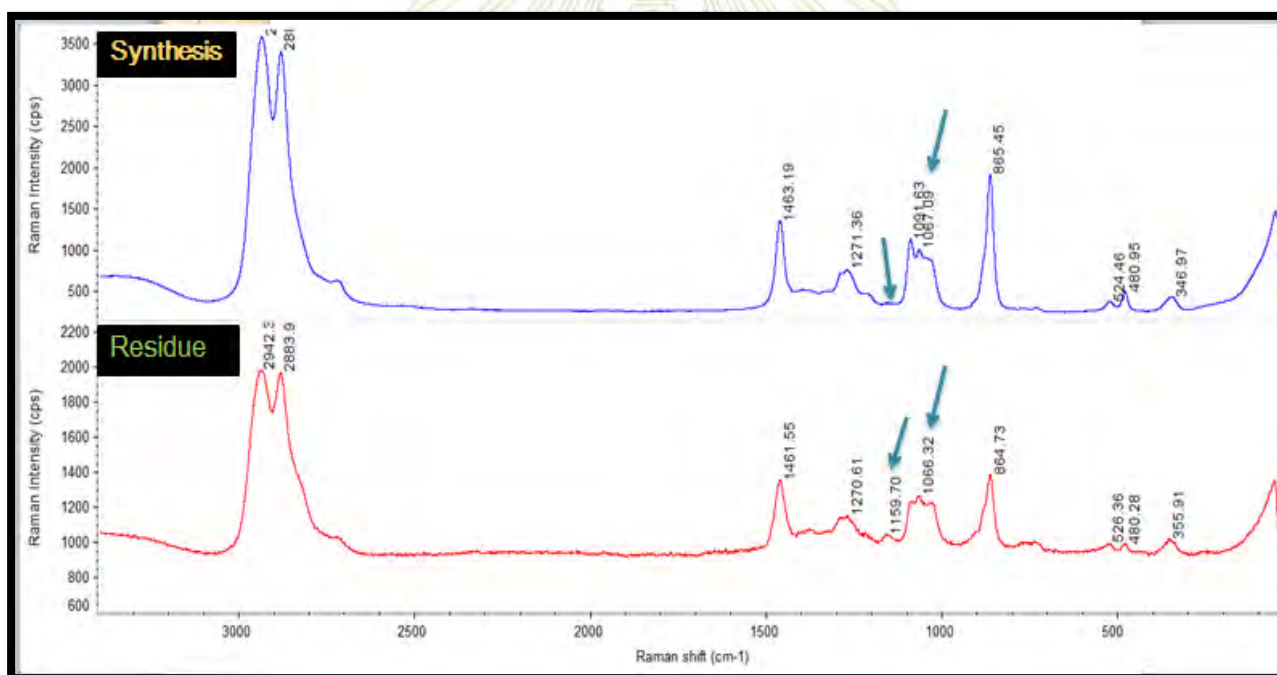


**Figure 35** Raman spectra of alumina and TEA reaction at  $197^{\circ}\text{C}$ , 2 h.

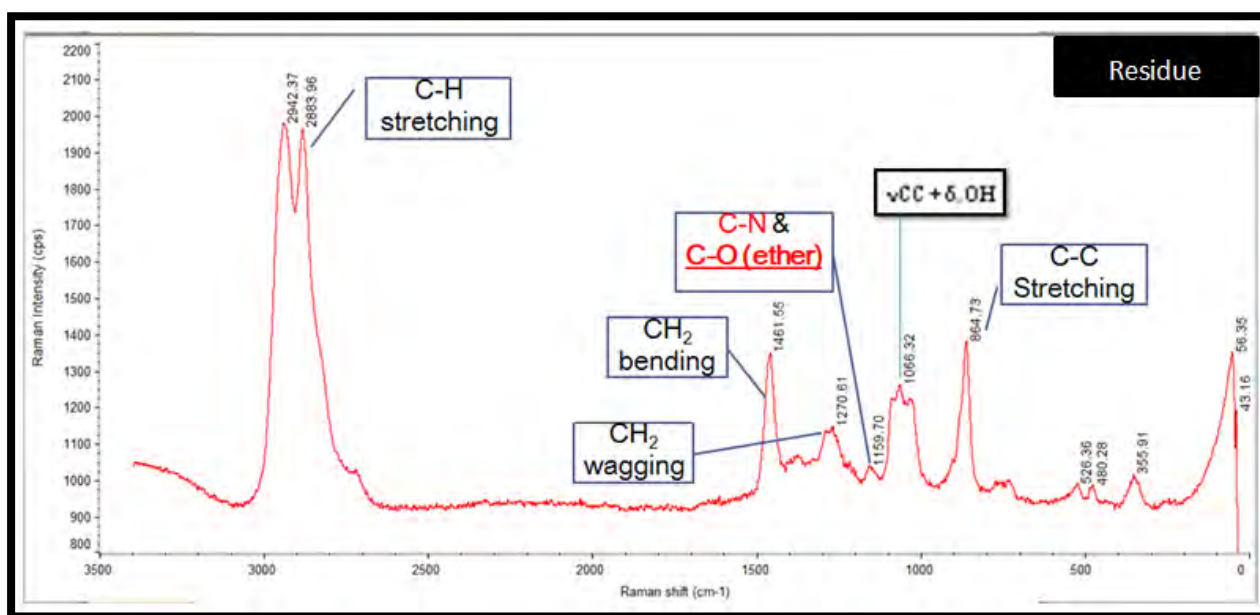


**Figure 36** Raman spectra of solution after reaction (residue) at 197°C, 2 h.

The NMR spectra of alumina and TEA reaction were shown in **Figure 37** and **38**. They showed that spectra of residue after reaction had new peaks at chemical shift 3.58(t,2H), 2.56(t,2H) and 4.70(broad), which identified as N-CH<sub>2</sub>-CH<sub>2</sub>-O-Al-OH, N-CH<sub>2</sub>-CH<sub>2</sub>-O-Al-OH and N-CH<sub>2</sub>-CH<sub>2</sub>-O-Al-OH of Al-TEA complex, respectively. The peak at 3.64(s, 4H) belongs to remaining ethylene glycol in mixture solution. The ratio of EG/TEA of solution before and EG/Al-TEA after reaction was calculated in **Figure 39** and **40**. Decreasing ratio can be described as the evaporation of EG. New peaks at 3.58 and 2.56 ppm shifted to higher chemical shift comparing with the peaks of pure TEA spectra because the bonding between Al and OH group which could act as electron withdrawing group. Moreover, new peak at 4.70 ppm shifted to lower chemical shift comparing with the peak of solution before reaction since OH attached with Al contributing to suggest Al-TEA complex shown in **Figure 41**. The structure of aluminate anion and TEA was verified by Raman and NMR evidence<sup>(22)</sup>.



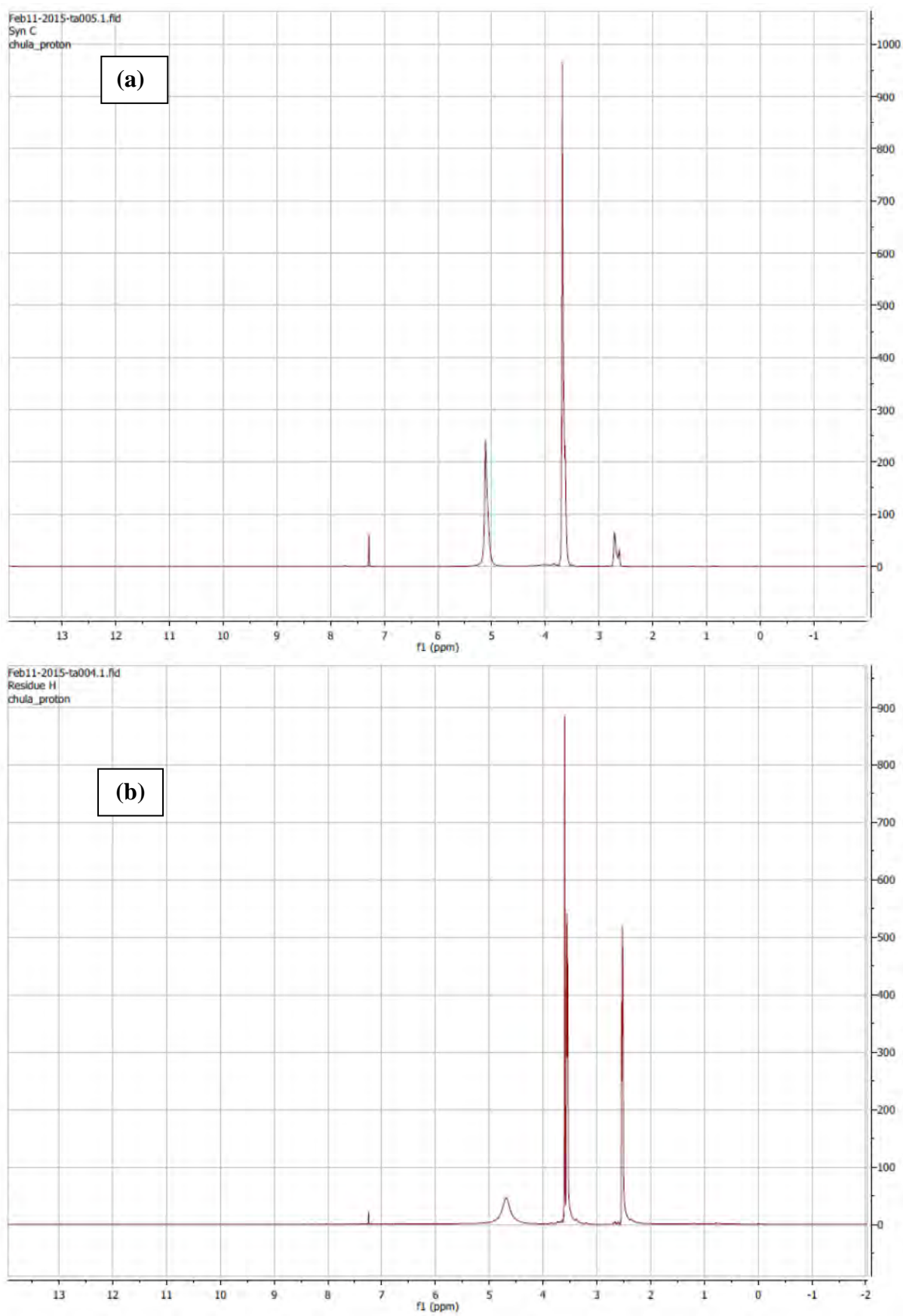


**Figure 37** NMR spectra (a) Solution before reaction, (b) Residue

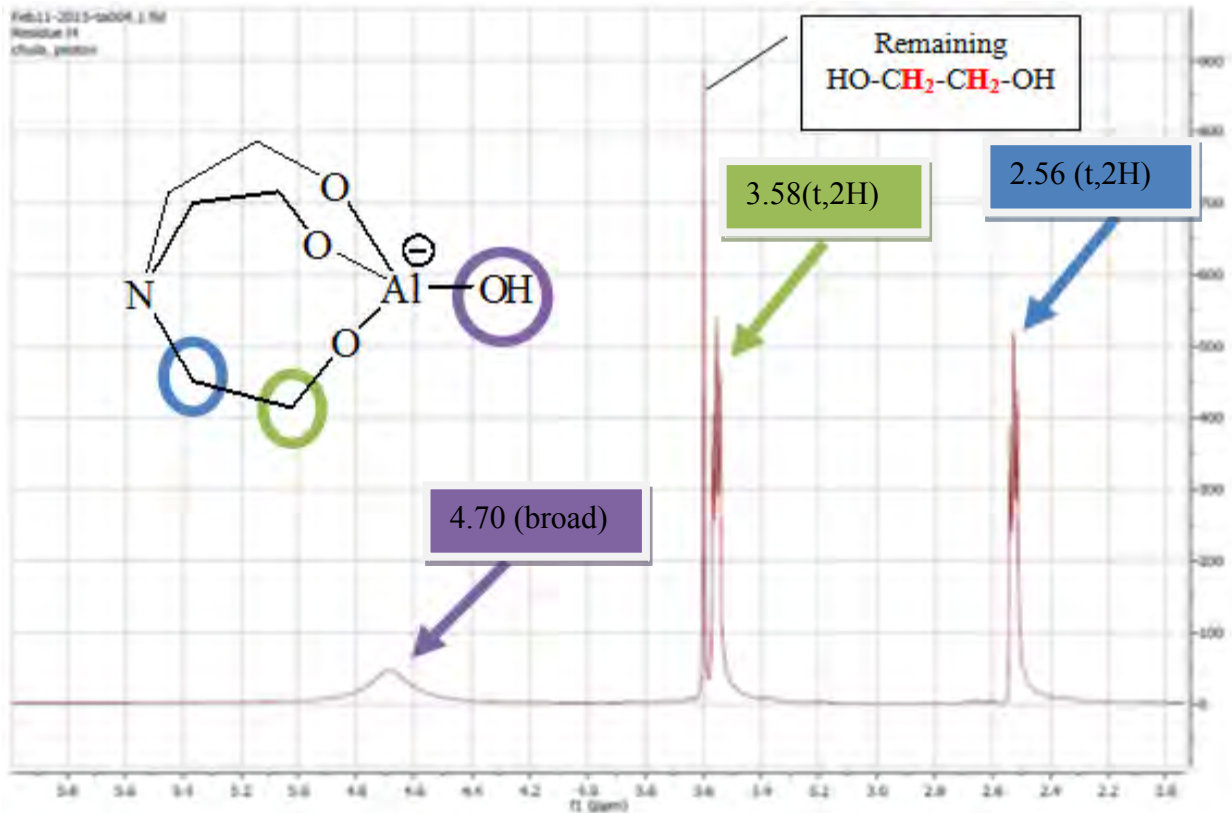


Figure 38 NMR spectrum of residue (Al-TEA complex) in range of 2-6 ppm

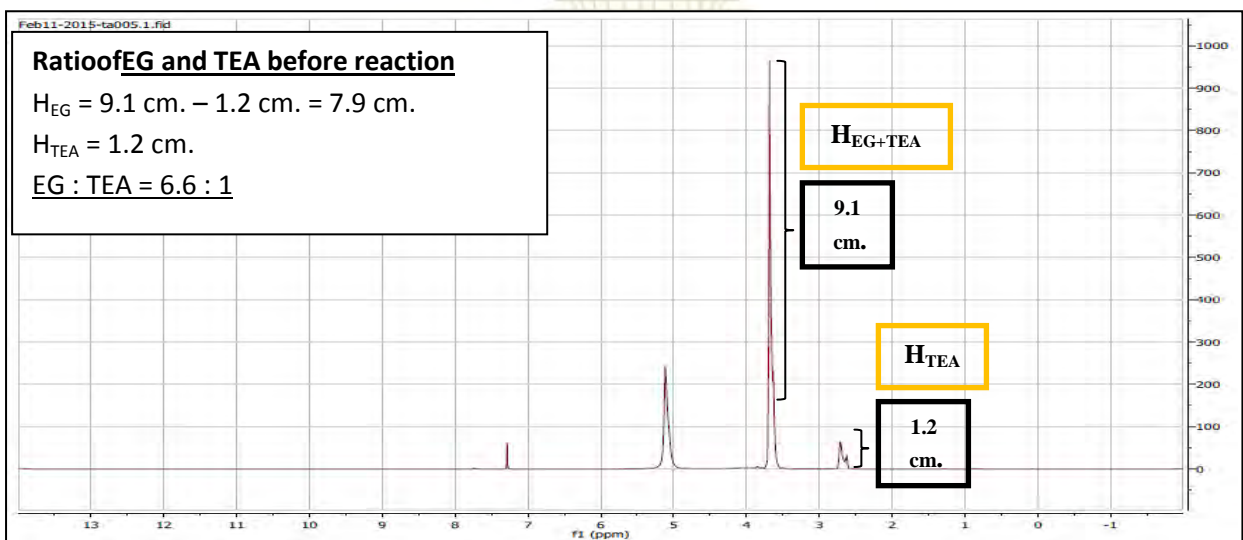
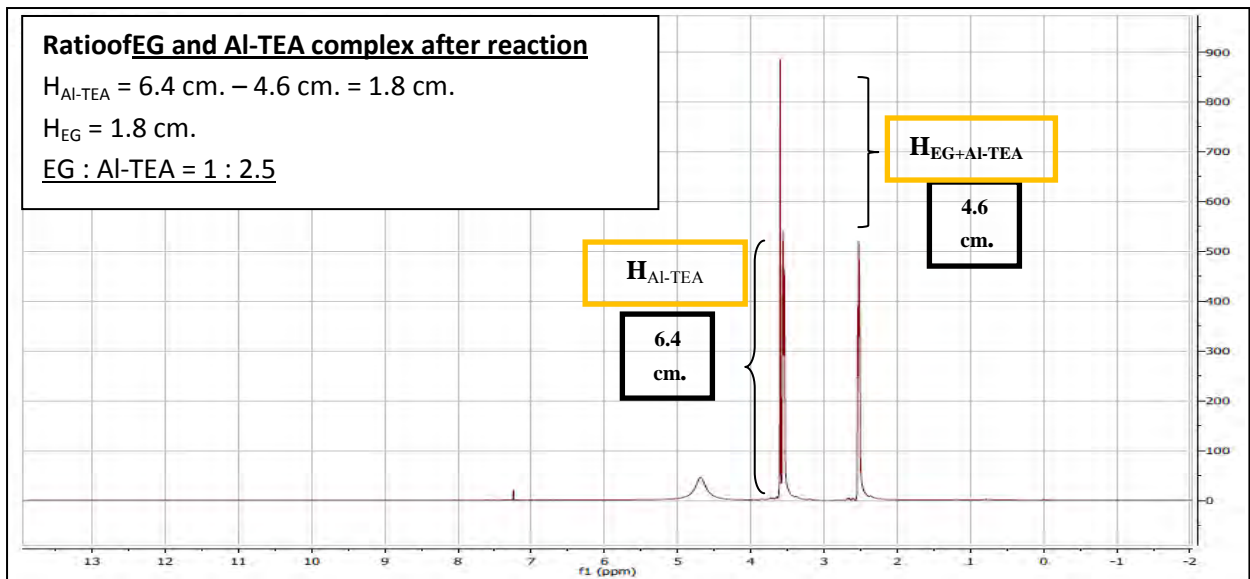
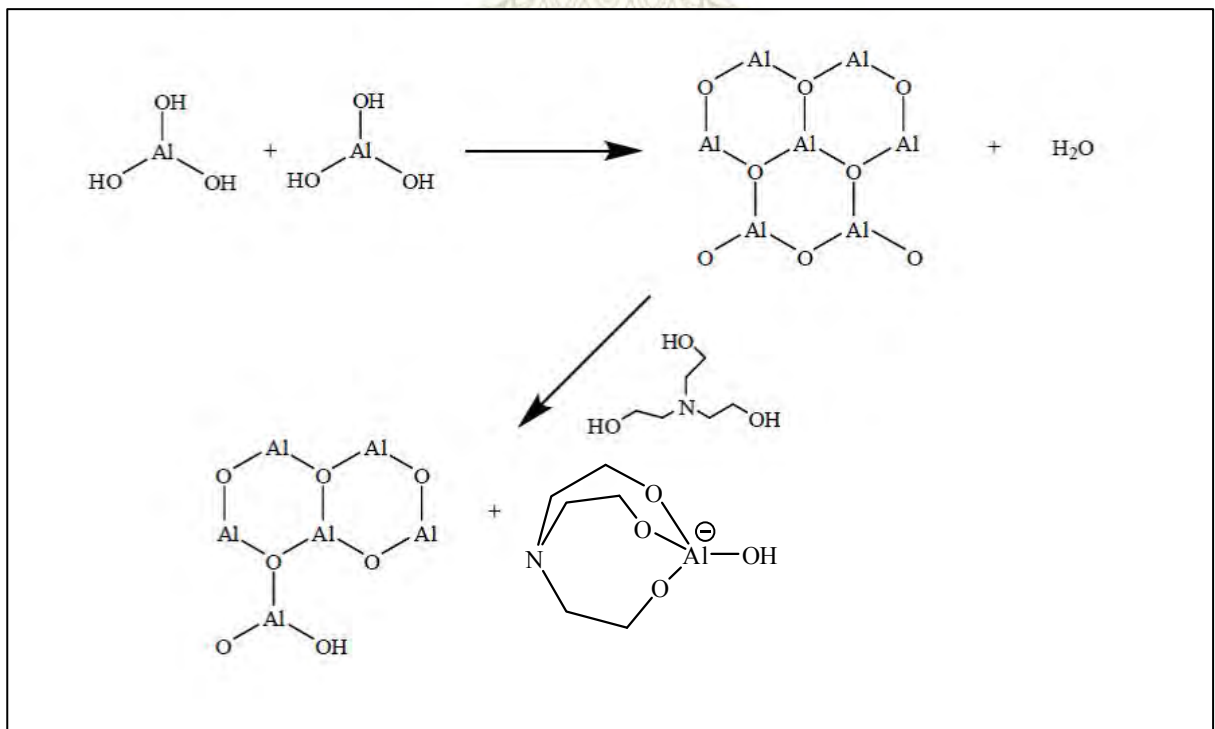


Figure 39 Calculation ratio of EG and TEA before reaction



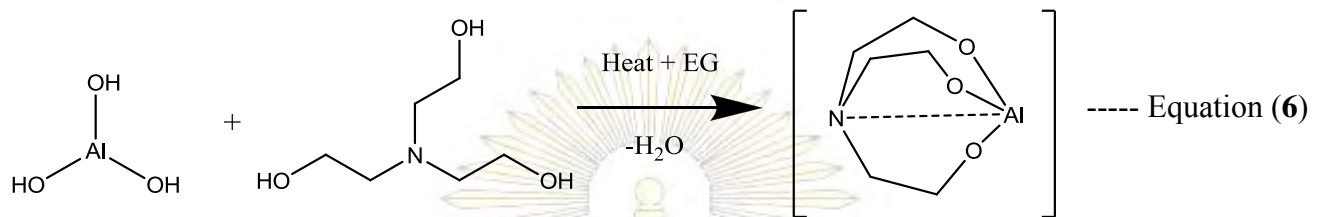
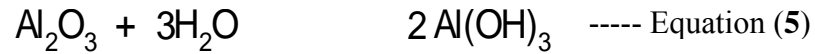
**Figure 40** Calculation ratio of EG and Al-TEA (after reaction)

According to results from Raman spectroscopy and NMR spectroscopy, TEA could remove alumina (corundum) that might cause from the nucleophilicity of TEA. Amine base, TEA, worked as nucleophile to increase the removal rate in lapping process by alumina removal in basicity solution to form Al-TEA complex as following suggested mechanism.



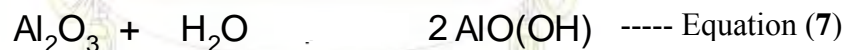
**Figure 41** The proposed structure of Al-TEA complex from alumina (powder) reaction experiment

Another pathway of mechanism might be occurred from both of alumina forms reacts with three water molecules in lubricant to form aluminum hydroxide or alumina trihydrate ( $\text{Al}_2\text{O}_3 \cdot 3\text{H}_2\text{O}$ ) in basic condition, then further reacted with TEA to form Al-TEA complex which is the same as the mechanism proposed as in equation<sup>(21)</sup>(5) and (6).



The different structure of Al-TEA and anion Al-TEA complex depend on pH of solution. If pH in reaction more than 8 and low concentration of alumina, the form of complex will exist in anion aluminate complex because this condition aluminum can form 3 bonds with TEA and another bond to hydroxide. This result was suggested relating to aluminum oxide phase diagram<sup>(2)</sup>.

The alumina recession is also caused by hydration layer from reaction between alumina and one molecule of water which can be removed easily by mechanical action following this equation<sup>(23)</sup>(7).



ภาควิชาเคมี  
คณะวิทยาศาสตร์  
จุฬาลงกรณ์มหาวิทยาลัย

### 3.5.3 Optical microscope and AFM of dipping coupon

The optical microscope results of square coupon dipped samples in different lube solutions were shown in **Figure 42**, **43** and **44**, respectively. The images of optical microscope show that coupon without dipping has some slightly defected from dust or contamination from the air. Coupon dipping in 0%-TEA is not found defect because it may be cleaned with lube. Finally, coupon dipping in 6%-TEA is found that some part of the AlTiC surface is lost and this lube provides the damage on surface. The results are relatively same for all magnification images. From 100x magnify power, the surface was found purple color of defect. It may be caused by the alumina layer which was peeling in dipping step. According to the results, TEA causes losing amorphous alumina layer by chemical removal reaction as described in above section (3.5.2) and also deteriorates coupon surface as well as leaving defect on it.

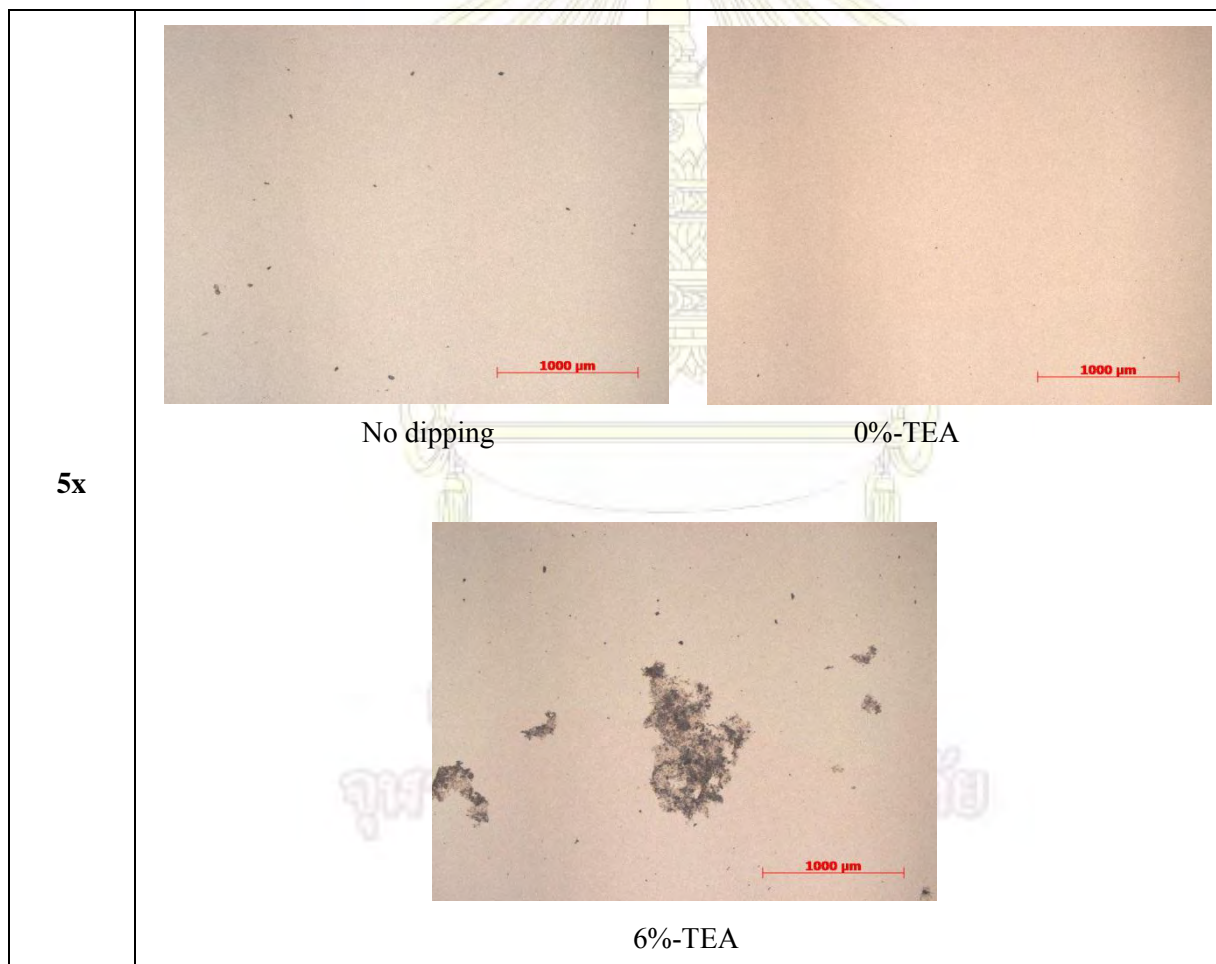


**Figure 42** Optical microscope images of square coupon dipped sample at 100°C, 4 h (5x)

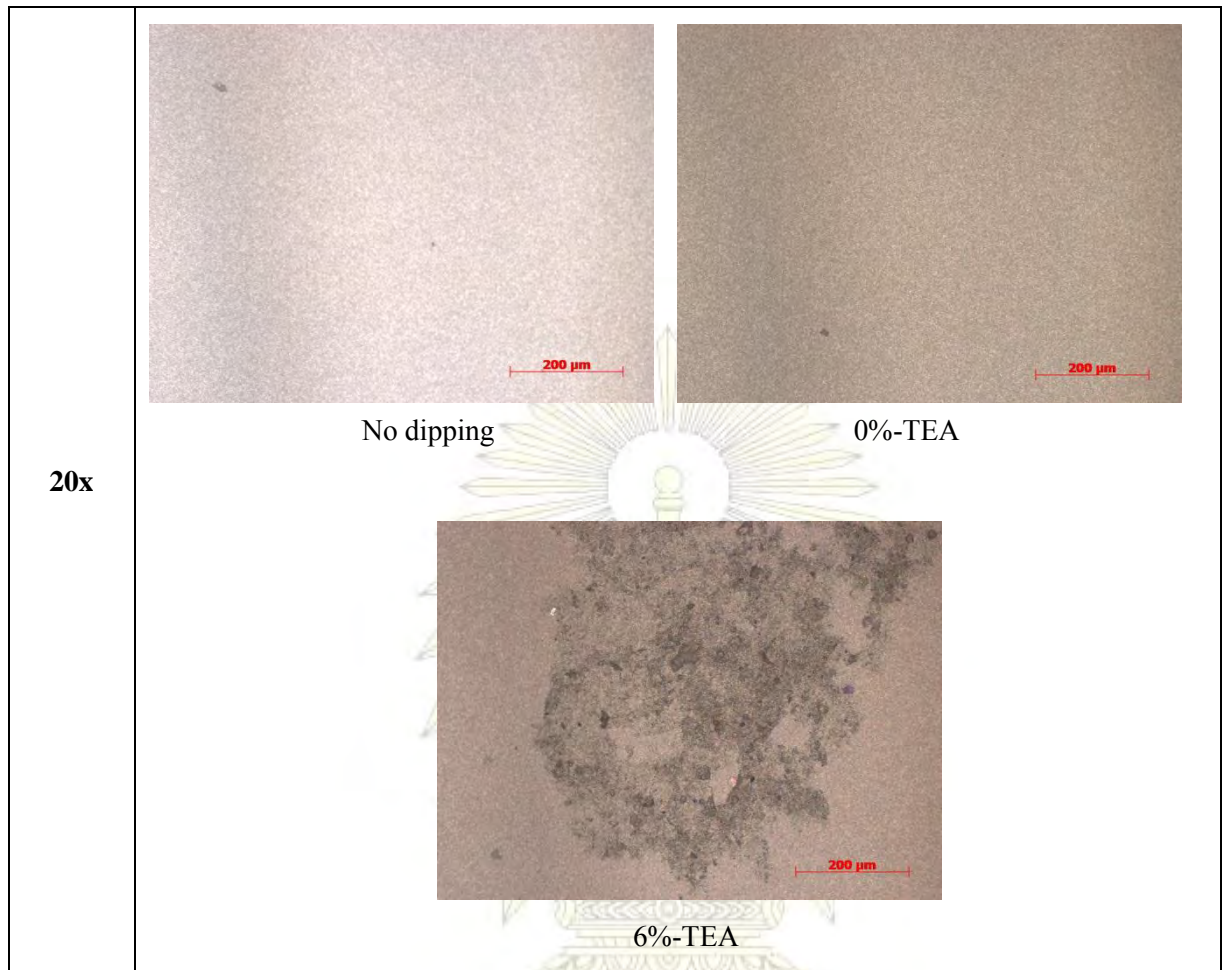


**Figure 43** Optical microscope images of square coupon dipped samples at different conditions(20x)

ภาควิชาเคมี  
คณะวิทยาศาสตร์  
จุฬาลงกรณ์มหาวิทยาลัย

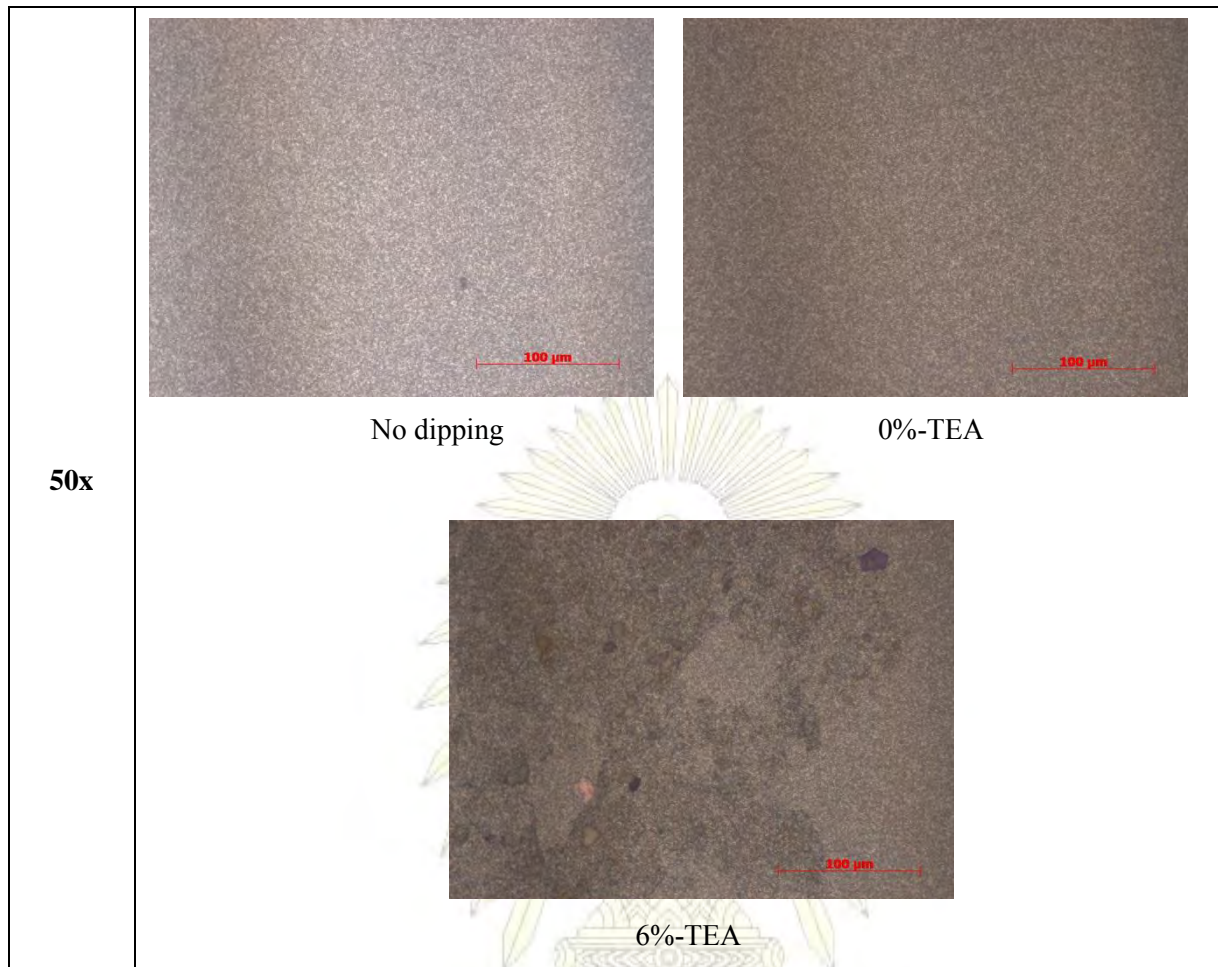


**Figure 44** Optical microscope images of square coupon dipped samples at different conditions (50x)

The atomic force micrograph images of AFM were shown in **Figure 45** and **46**. Similarly to the results of images from optical microscope, 2D AFM images present the significantly different of the surface dipped in 6%-TEA comparing to 0%-TEA and no dipping. Dipping in 6%-TEA image showed two different surface layers. So, TEA reacts with alumina layer on surface as a result of losing out of amorphous alumina. According to the data from roughness test in **Table 14**, the step height value is 12.28 nm which indicated the height of removed alumina layer. Nevertheless, the roughness values ( $R_a$ ) were not significantly different due to small thickness of alumina layer coated on AlTiC. The 3D images of AFM also showed the difference of two layers.

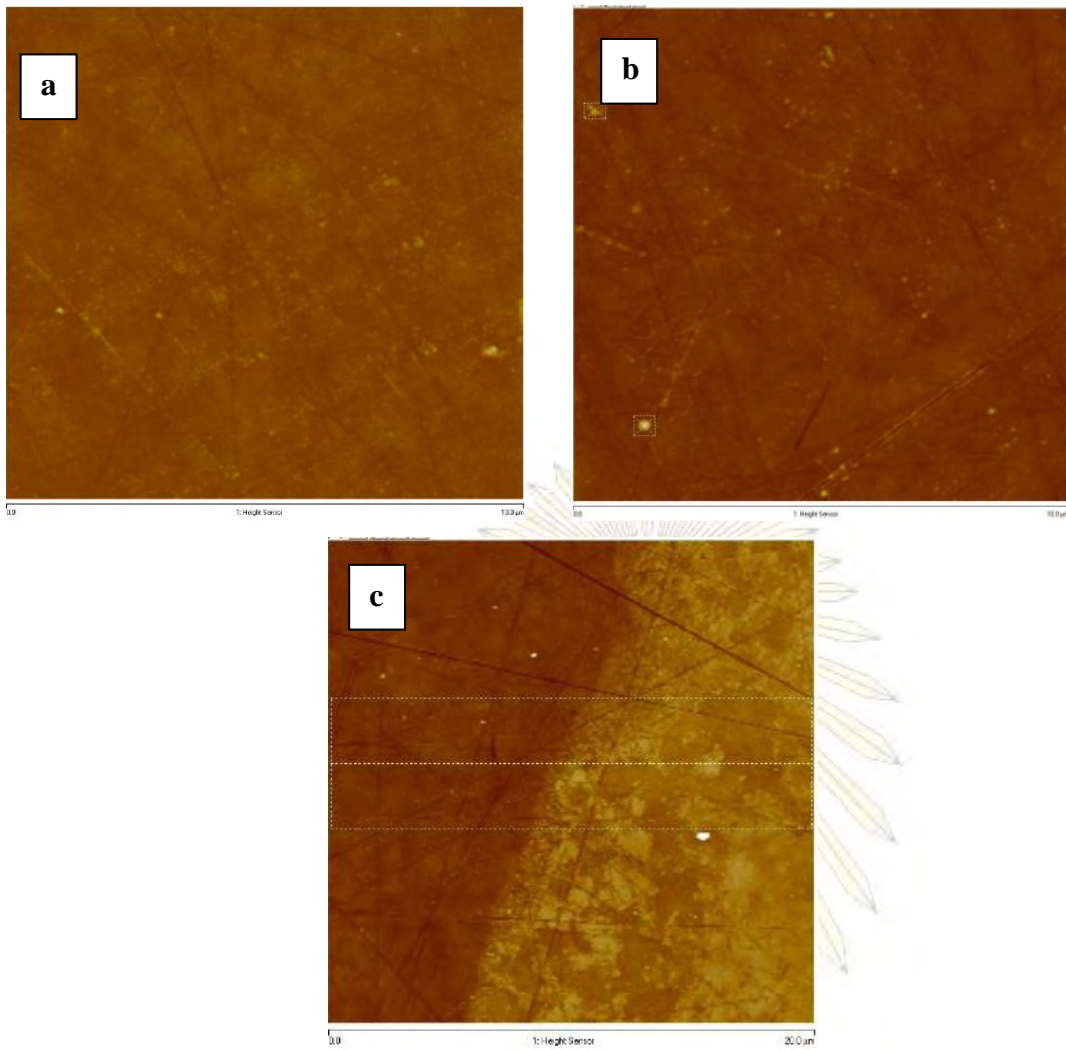


**Figure 45** AFM images of square coupon dipped sample at different conditions (a) No dipping (b) Dipping in 0%-TEA (c) Dipping in 6%-TEA

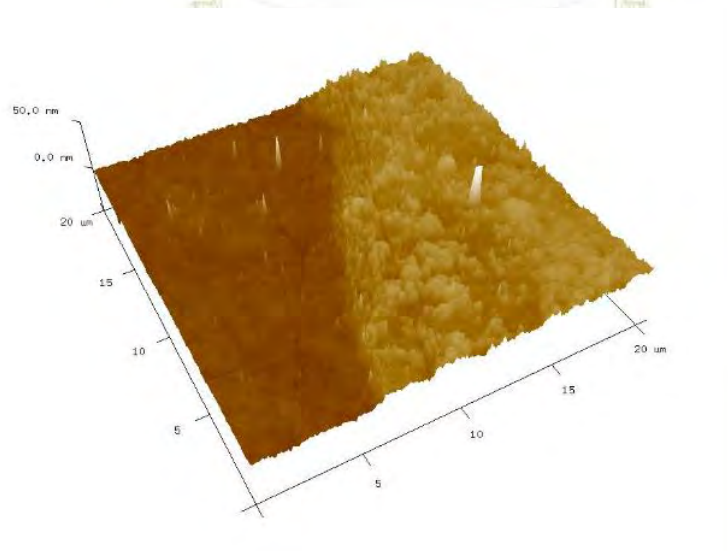


**Figure 46** 3D AFM image of square coupon dipped in 6%-TEA



**Table 14** Roughness test of dipping coupon in each lube.

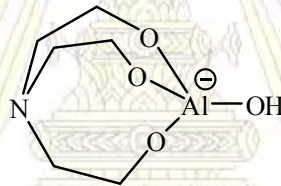
Coupon dipped in	Point #	Front side (nm)			Step height (nm)
		R <sub>a</sub>	R <sub>q</sub>	R <sub>max</sub>	
No dipping	#1	1.020	1.450	32.60	
	#2	1.030	1.430	39.60	
	#3	0.998	1.360	24.20	
	#4	1.240	1.780	32.80	
0%-TEA	#1	0.969	1.410	28.80	
	#2	0.940	1.340	25.00	
	#3	0.978	1.470	26.40	
	#4	0.863	1.170	19.10	
6%-TEA	#1	1.400	1.930	46.10	
	#2	1.400	1.820	27.90	
	#3	0.885	1.170	22.60	
	#4	1.000	1.380	31.00	
	S				12.28



## Chapter 4

### Conclusion

TEA, one of the additives in lubricant, was a major influence to increase pH and TBN due to amine base functional group and also rising viscosity. The basicity of lubricant had also impact on lapping time. From lapping and dipping experiments, adding more %TEA reduced lapping time since the combination of mechanical along with chemical removal from rising viscosity and particular chemical reaction of alumina and TEA. The result found that 6%TEA in EG base stock was an alternative to use in final lapping process because it gave highest alumina recession which is major slider head substrate and also decreasing lapping time. However, 10%TEA did not significantly increase lapping time and not provide the most alumina recession because at 10%TEA cannot completely dissolve in EG. Moreover, increasing to 6%TEA provides most corrosion rate of cobalt and iron acted as representative of slider bar because alumina is not suitable for corrosion test since it is a non-conductive material. Alumina was removed in lubricant containing TEA by reaction to form intermediate complex of Al-TEA. According to alumina reaction experiment, the characterization results from NMR and Raman spectra suggested that Al-TEA is formed as the following structure.



Images from optical microscope implied that TEA removed alumina layer on AlTiC substrate. From the observation, alumina layer was peeled out of surface and TEA also caused surface damage after dipping. According to the data from roughness test, the step height value is 12.28 nm which indicates the height of removed alumina layer relative to AlTiC base. AFM images showed significantly difference when dipping in both of 0%-TEA and 6%-TEA. The alumina layer of surface dipping in 6%-TEA was peeled out of surface due to effect of TEA. For suggestion, scanning electron microscope should be done for further observation.

คณะวิทยาศาสตร์  
จุฬาลงกรณ์มหาวิทยาลัย

## References

- [1] Frank Talke's Tribology and Mechanics Lab." *Hdd-intro*. Professor Frank and His Team. Web. Accessed on 2 Feb. 2015. <<http://talkelab.ucsd.edu/index.php/hdd-intro>>.
- [2] Jiang, M.; Hao S.; Komanduri R. On the Advanced Lapping Process in the Precision Finishing of Thin-film Magnetic Recording Heads for Rigid Disc Drives. *Materials Science & Processing*. **2003**, 77, 923-932.
- [3] John, P.; Neville,; Peterson & Williams, Black ceramic substrates, HQ 96484, New York, **2002**
- [4] Vashishta, P.; Rajiv K. Kalia, Aiichiro a kano, and Jos Pedr o i no. Interaction Potentials for Alumina and Molecular Dynamics Simulations of Amorphous and Liquid Alumina. *Journal of Applied Physics*. **2008**, 103, 83504.
- [5] Advanced Ceramic Technologies & Products. Tokyo: Springer, **2012**. 227-230.
- [6] Wiberg, E.; Holleman, A.F. Inorganic Chemistry, *the journal of Elsevier*, **2001**.
- [7] Lee, S.K.; Lee, S.B.; Park, S.Y.; Yi, Y.S.; Ahn, C.W.. Structure of amorphous aluminium oxide. *Phys. Rev. Lett.* **2009**, 103, 095501
- [8] Marinescu, Ioan D. Handbook of Lapping and Polishing. Boca Raton, FL: CRC, **2007**.
- [9] Supavasuthi, C., Fernandez, B.L., Tan, S., Sukasem, P. Handbook of the Final Lapping Process. Western Digital (Thailand) Co., Ltd., **2013**.
- [10] Stachowiak, G. W., and A. W.. Batchelor. Engineering Tribology. 3rd ed. Amsterdam: Elsevier Butterworth-Heinemann, **2005**.
- [11] Caines, A. J., and R. F. Haycock. Automotive Lubricants Reference Book. 2nd ed. Warrendale, PA: SAE International, **2004**.
- [12] S. Boyde, Green lubricants-Environmental benefits and impacts of lubrication, *Green Chem.* **2002**, 2, 293-307.
- [13] P.V. Snyder, GTL lubricants: The next stop, NPRA Lubricants and Waxes Meeting, Houston, **1999**.
- [14] E.D. Sowle, T.M. Lachocki, Linear dialkylbenzenes as synthetic base oils, *Lubric. Engng.*, **1996**, 52, 116-20.
- [15] A. Pettersson, High-performance base fluids for environmentally adapted lubricants, *Tribol. Intl.* **2007**, 40
- [16] S. Bhuyan, S. Sundarajan, L. Yao, E.G. Hammond, T. Wang, Boundary lubrication properties of lipid-based compounds evaluated using microtribological methods, *Tribol.Lett.* **2006**, 22, 67-72.

- [17] Rudnick, Leslie R. *Lubricant Additives Chemistry and Applications*. 2nd ed. Boca Raton, FL: CRC, **2009**.
- [18] Wills, J. George. *Lubrication Fundamentals*. 2nd ed. New York: M. Dekker, **1980**.
- [19] Dow Chemical Company (1998) *The Specifier's Guide to Buying and Applying Ethanolamines*, Midland, MI
- [20] V.S. Muralidharan, M. Veerashanmugamani, G. Paruthimalkalaigan, Ethanolamines as corrosion inhibitors for pure nickel in sulphuric acid solution. *Electrochemistry*, **1985**, 4, 373-375.
- [21] R. Baranwal, M.P. Villar, R. Garcia, R.M. Laine, Flame Spray Pyrolysis of Precursors as a route to nano-mullite powder: powder characterization and sintering behavior. *Journal of the American Ceramic Society*, **2001**, 84, 951-961.
- [22] D.A. Palmer, P. Bénézech, D.J. Wesolowski, S. Hilic, Experimental studies of the solubilities of aluminum oxy-hydroxy phases to 300°C. 34<sup>th</sup> Annual Hydrometallurgical Meeting, Banff, Canada, October 23-28, **2004**.
- [23] Kim, H., Manivannan R., D. Moon, H. Xiong, J.P., Evaluation of double sided lapping using a fixed abrasive pad for sapphire substrates. *Wear*, **2013**, 203, 1340-1344.
- [24] Khaled, K.f., Abdel-Rehim S.s., Sakr G.b. "On the Corrosion Inhibition of Iron in Hydrochloric Acid Solutions, Part I: Electrochemical DC and AC Studies. *Arabian Journal of Chemistry*, **2012**, 5, 213-218.
- [25] Keith, Lawrence H. *The National Toxicology Program's Chemical Data Compendium*. 2nd ed. Boca Raton: Lewis, 1992. 751.
- [26] Cao, J.g., Shen, M., Zhou L.w. "Preparation and Electrorheological Properties of Triethanolamine-modified TiO<sub>2</sub>. *Journal of Solid State Chemistry*. **2006**, 197, 1565-568.
- [27] Y.H. Yu, Y.Y. Lin, C.H. Lin, C.C. Chan, Y.C. Huang. High-performance polystyrene/graphene-based nanocomposites with excellent anti-corrosion properties. *Polymer Chemistry*. **2013**, 5, 535.
- [28] Y. Wen, H. Zhang, P. Qian, H. Zhou, P. Zhao, B. Yi, Y. Yang, A Study of the Fe(III)/Fe(II)-triethanolamine complex redox couple for redox flow battery application. *Electrochimica Acta*, **2012**, 81, 769-775.
- [29] Effect of conductivity on corrosion  
Accessed on 2 Feb. 2015 <<https://www.usc.edu/CSSF/History/2009/Projects/S0516.pdf>>
- [30] S. Kurtaran, Vibrational frequencies and structural determination of triethanolamine and diethanolamine by density functional theory calculations. *Book of Abstracts*, **2008**, 764.

- [31] G. Socrates, G. Socrates, Infrared and Raman Characteristic Group Frequencies: Tables and Charts. 3rd ed. Chichester: Wiley, **2001**.
- [32] S.G. Skoulika, C.A. Georgiou, M.G. Polissiou "Rapid Quantitative Analysis of organophosphorus pesticide formulations by FT-Raman spectroscopy", Internet J. Vib. Spec.[www.ijvs.com] 4, 3, 4, **2000**.
- [33] Krishnan, K.R.; Krishnan, S..Raman and infrared spectra of ethylene glycol. *Proceeding of the Indian Academy of Sciences*.**1966**, 2, 111-122





# Appendix

ภาควิชาเคมี  
คณะวิทยาศาสตร์  
จุฬาลงกรณ์มหาวิทยาลัย

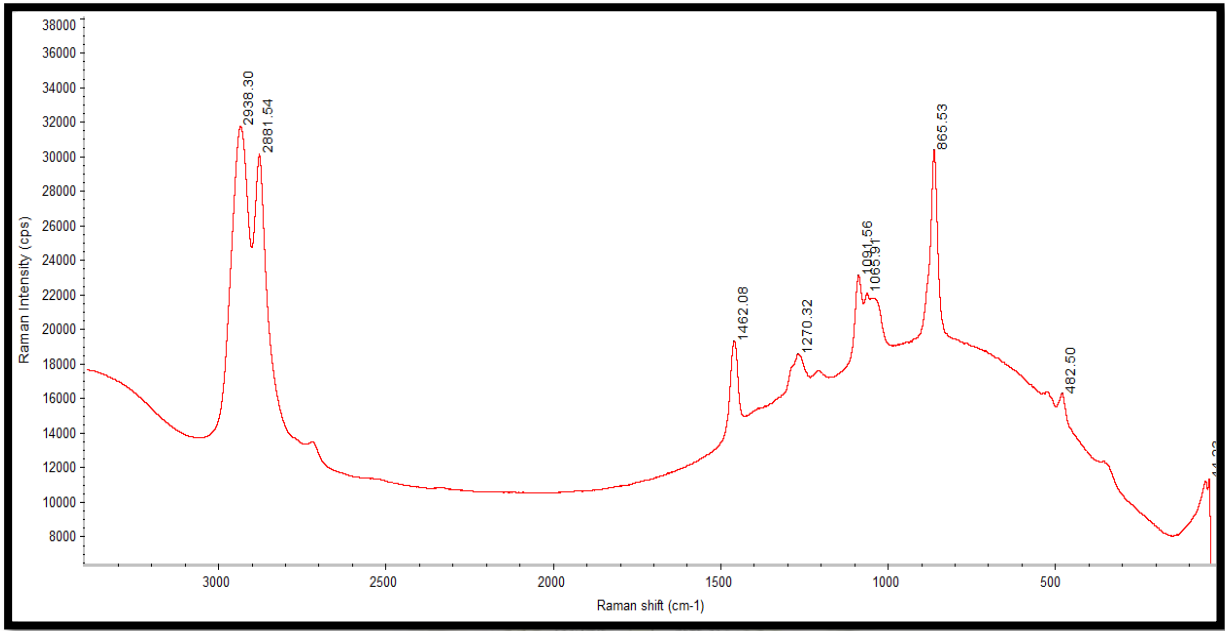


**Figure 1** Raman spectra of Ethylene glycol

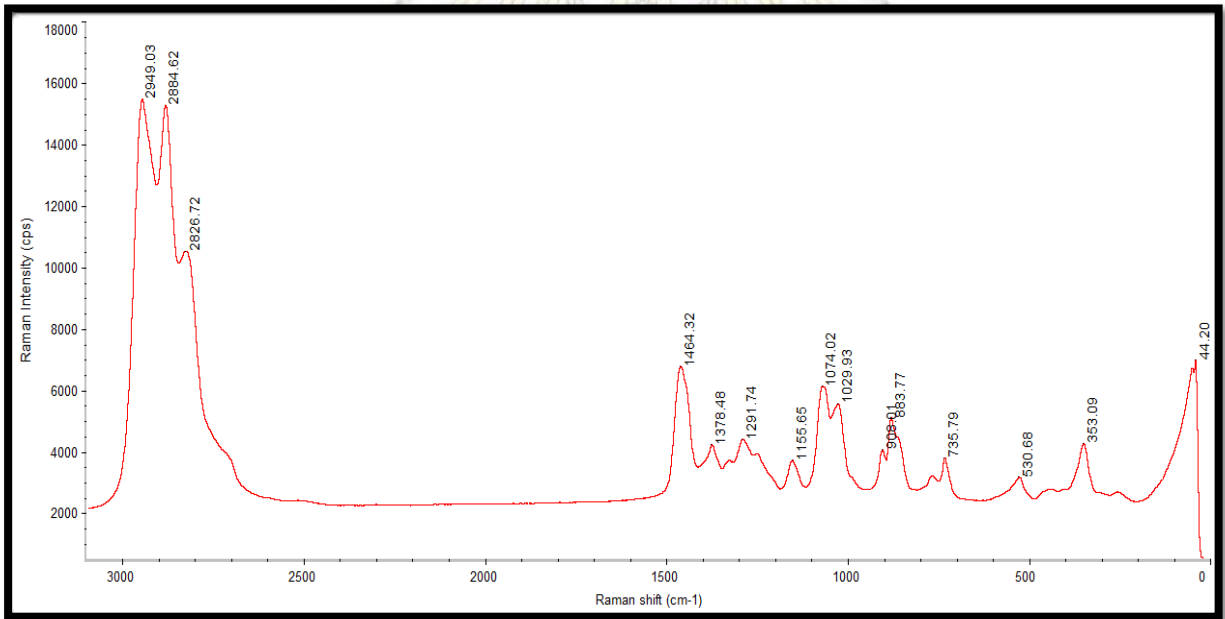


**Figure 2** Raman spectra of Triethanolamine

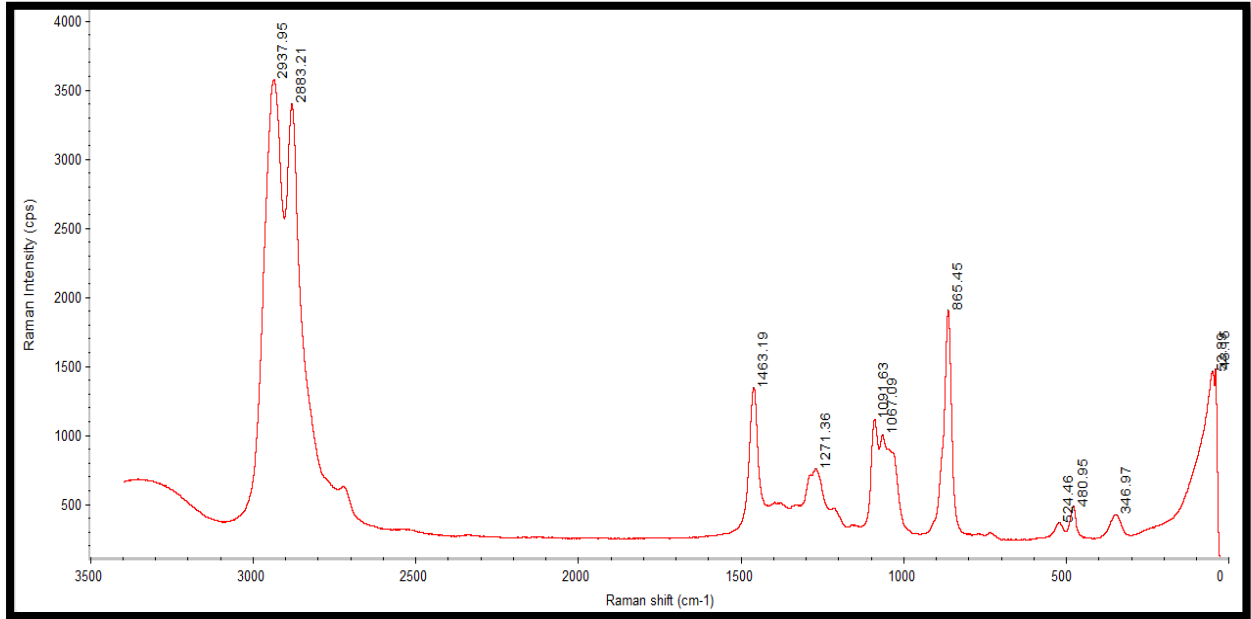


**Figure 3** Raman spectra of solution before reaction (synthesis)

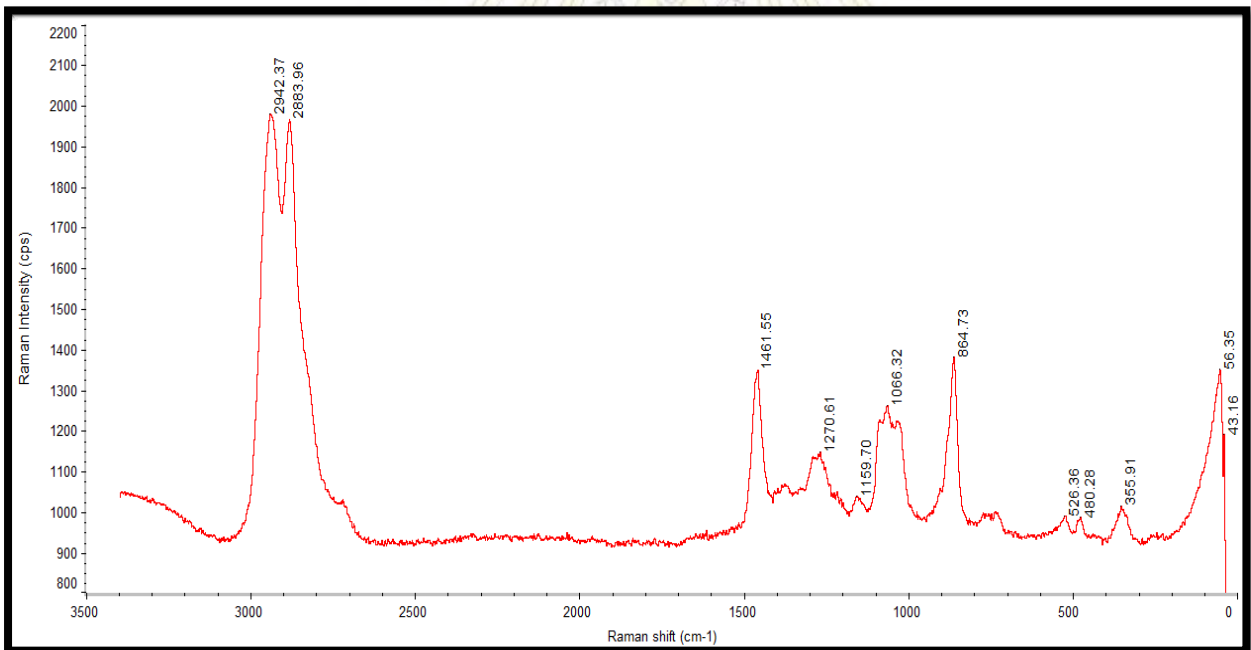


**Figure 4** Raman spectra of solution after reaction (residue)



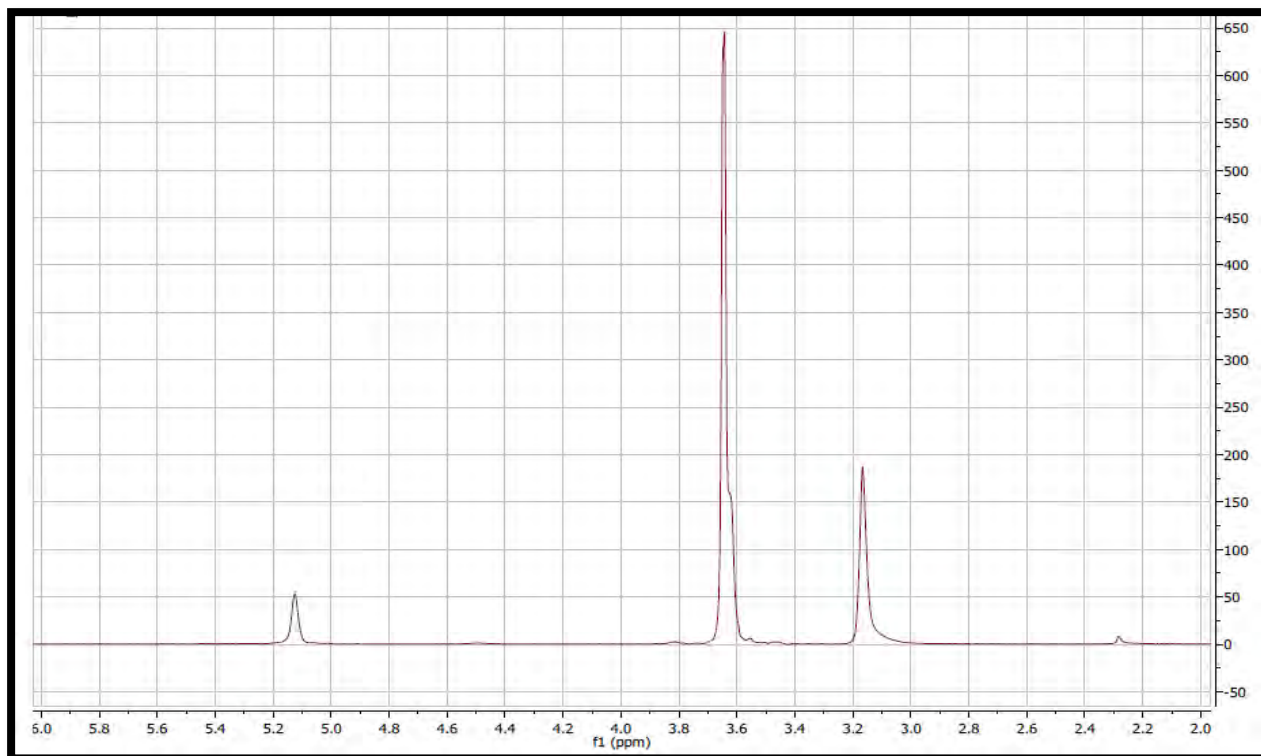


**Figure 5**  $^1\text{H-NMR}$  (400 MHz,  $\text{CDCl}_3$ ) spectra of Ethylene glycol

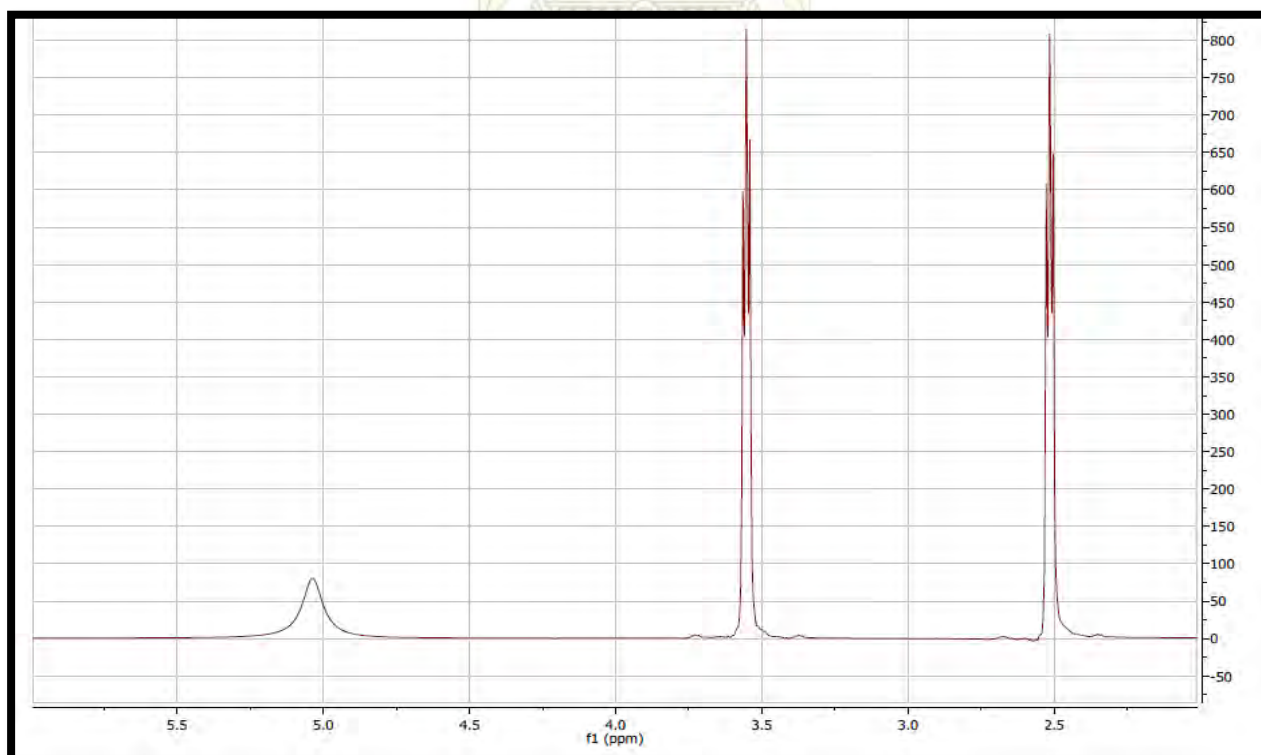


**Figure 6**  $^1\text{H-NMR}$  (400 MHz,  $\text{CDCl}_3$ ) spectra of Triethanolamine

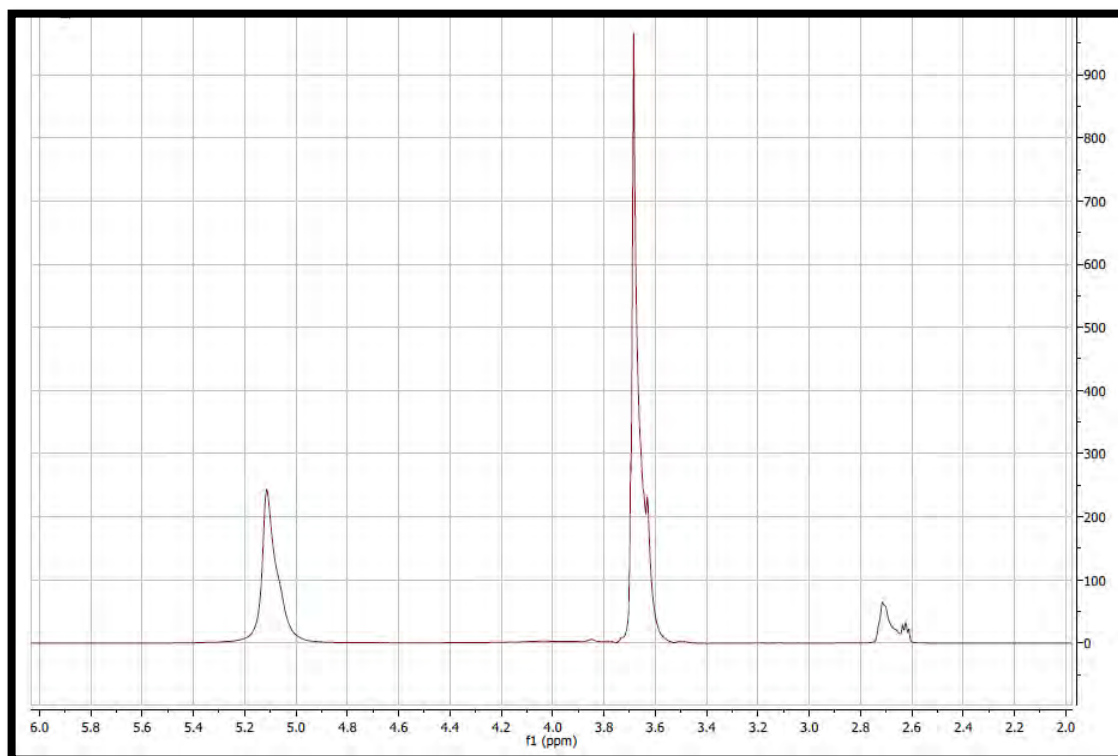


**Figure 7**  $^1\text{H-NMR}$  (400 MHz,  $\text{CDCl}_3$ ) spectra of solution before reaction (synthesis)

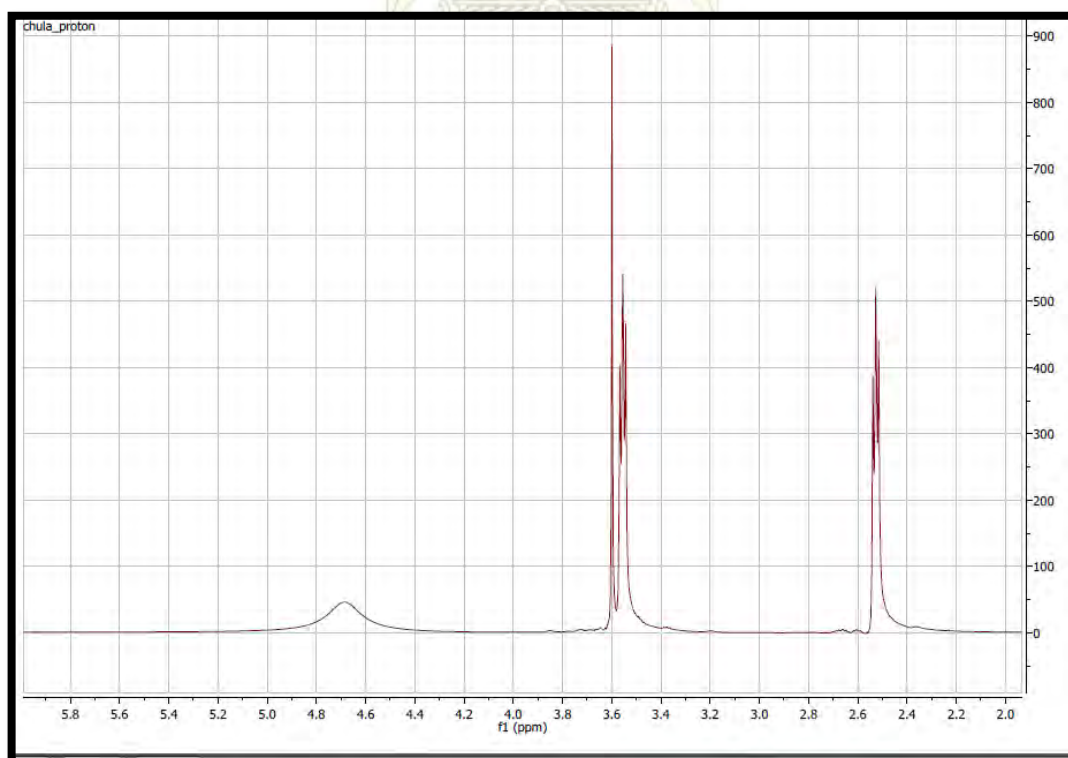


**Figure 8**  $^1\text{H-NMR}$  (400 MHz,  $\text{CDCl}_3$ ) spectra of solution after reaction (residue)

## VITA

PiyananDangnearm was born on October 31, 1993 in Chonburi, Thailand. He graduated from RatwinitBangkaewschool in 2010. Then, he attended Chulalongkorn University as an undergraduate student in the Bachelors of Science in chemistry programs. During his final year, he had an opportunity to complete the internship and the senior project at Western Digital Co, Ltd. for 3 months. After graduating, he had interest for further study in the field of analytical chemistry at ChulalongkornUniversiry.

Contact information: House No.226/3, Village No.1, Bangbo district, Bangbo sub-district, Samutprakarn province.

